Post-irradiation Heating Tests of As-irradiated AGR-3/4 TRISO Fuel Compacts

INL/RPT-24-80477

AGR TRISO Fuel Qualification – Next Generation Fuels

M3TG-24IN04020317

SEPTEMBER 2024

John D. Stempien
Lu Cai

Idaho National Laboratory

Idaho National Laboratory

Battelle Energy Alliance manages INL for the U.S. Department of Energy's Office of Nuclear Energy

INL/RPT-24-80477

Post-irradiation Heating Tests of As-irradiated AGR-3/4 TRISO Fuel Compacts

M3TG-24IN04020317

John D. Stempien
Lu Cai
Idaho National Laboratory

SEPTEMBER 2024

Idaho National Laboratory
Idaho Falls, Idaho 83415

http://www.inl.gov

Prepared for the
U.S. Department of Energy
Office of Nuclear Energy
Under DOE Idaho Operations Office
Contract DE-AC07-05ID14517

Page intentionally left blank

INL ART Program

Post-irradiation Heating Tests of As-irradiated AGR-3/4 TRISO Fuel Compacts

INL/RPT-24-80447

September 2024

Approved by:

Paul Demkowicz — 9/6/2024

Paul A. Demkowicz, PhD
ART AGR Fuels Technical Director — Date

Travis Mitchell — 9/5/2024

Travis R. Mitchell
ART AGR Program Manager — Date

MJ Sharp — 9/9/2024

Michelle T. Sharp
INL Quality Assurance — Date

Page intentionally left blank

ABSTRACT

Four post-irradiation heating tests of fuel compacts from the U.S. Advanced Gas Reactor (AGR)-3/4 irradiation experiment were completed. In addition to tristructural isotropic (TRISO)-coated driver fuel, each compact contained designed-to-fail (DTF) particles with fuel kernels coated only in pyrocarbon so as to simulate exposed kernels. Tests at 1600/1700°C, 1400°C, and 1200°C were performed to measure fission product release as a function of time and temperature. Silver release was highest in the 1200°C test, supporting the observation that silver release rates are highest in the 1100–1300°C range. Compared to tests of AGR-1 compacts with no exposed kernels, the Cs-134 and Kr-85 releases were noticeably higher in AGR-3/4. The exposed kernels' contributions to Eu and Sr release are inconclusive, due to the difficulty in distinguishing among the combined effects of higher irradiation temperatures in these particular AGR-3/4 compacts, the presence of the DTF particles, and the Fuel Accident Condition Simulator (FACS) test temperatures. These data can be used to make inferences about fission product retention in exposed kernels as a function of time and temperature.

Page intentionally left blank

ACKNOWLEDGMENTS

Cad Christensen was the process engineer responsible for operating the Fuel Accident Condition Simulator (FACS) furnace. Dr. Edward Reber operated and analyzed the spectra from the fission gas monitoring (FGMS) system. Support from staff at the Hot Fuel Examination Facility (FACS furnace operation) and Analytical Laboratory (condensation plate Sr-90 analysis) in regard to measuring the condensation plates is gratefully acknowledged. The authors are grateful for the reviews and feedback received from Dr. Paul Demkowicz that helped improve this report.

Page intentionally left blank

CONTENTS

FIGURES

TABLES

Page intentionally left blank

ACRONYMS

AGR	Advanced Gas Reactor
ATR	Advanced Test Reactor
DTF	designed-to-fail
EOI	end of irradiation
FACS	Fuel Accident Condition Simulator
FGMS	fission gas monitoring system
FIMA	Fissions per initial metal atom
HTGR	High-temperature gas-cooled reactor
INL	Idaho National Laboratory
IPyC	Inner pyrolytic carbon
M/C	Measured-to-calculated ratio
NRAD	Neutron Radiography
OPyC	outer pyrolytic carbon
PIE	post-irradiation examination
RDLBL	radial deconsolidation-leach-burn-leach
SiC	silicon carbide
TA	time-average
TAVA	time-average volume-average
TRISO	tristructural isotropic

Page intentionally left blank

Post-irradiation Heating Tests of As-irradiated AGR-3/4 TRISO Fuel Compacts

1. INTRODUCTION

The U.S. Department of Energy's Advanced Gas Reactor (AGR) fuel development and qualification program has fabricated and irradiated tristructural isotropic (TRISO)-coated particle fuels for high-temperature gas-cooled reactors (HTGRs). Four campaigns of fuel fabrication and irradiation in the Advanced Test Reactor (ATR) at Idaho National Laboratory (INL) have already been completed (Grover, Maki and Petti 2010; Grover and Petti 2014; Collin et al. 2018; Pham et al. 2021). In chronological order, those experiments were titled AGR-1, AGR-2, AGR-3/4, and AGR-5/6/7. Both destructive and non-destructive post-irradiation examination (PIE) of AGR-1 and AGR-2 are complete (Demkowicz et al. 2015a, Stempien et al. 2021a), and PIE of AGR-3/4 and AGR-5/6/7 is in progress.

Whereas AGR-1 and AGR-2 were intended to demonstrate the performance of high-quality TRISO fuel and to quantify the very low rates of silicon carbide (SiC) and TRISO coating failure, the AGR-3/4 irradiation experiment was designed to investigate the release of fission products from exposed fuel kernels and the migration of these fission products in fuel compact graphitic matrix and structural graphite materials. This area of study is necessary for refining fission product transport models and supporting reactor source-term calculations. As part of AGR-3/4 PIE, post-irradiation heating tests were conducted on AGR-3/4 fuel compacts in the Fuel Accident Condition Simulator (FACS) furnace at INL to study fission product release from exposed fuel kernels and fission product transport in the compact matrix under a range of temperatures representative of both normal reactor operation and postulated reactor accidents. These compacts were then subjected to post-heating destructive examinations via radial deconsolidation-leach-burn-leach (RDLBL) (Hunn et al. 2020; Helmreich et al. 2022; Stempien and Cai 2024b). Additional information on the RDLBL process, including its development and application to as-irradiated compacts is available in several other reports (Helmreich, Montgomery, and Hunn 2015; Stempien 2017; Helmreich et al. 2021; Stempien and Cai 2024a).

1.1. AGR-3/4 Fuel Description

AGR-3/4 was primarily a fission product transport experiment that consisted of fuel compacts containing about 1,898 TRISO-coated driver-fuel particles (similar to the AGR-1 baseline fuel) (Collin 2015a; Hunn and Lowden 2007; Hunn et al. 2014), along with precisely 20 designed-to-fail (DTF) particles that were intended to release fission products during irradiation.

The DTF particles served as a known source of fission products that migrated radially outward in the compacts and into the surrounding concentric rings of graphite and/or matrix material. Intact DTF particles were expected to behave like TRISO particles with a failed SiC layer (releasing substantial Cs but retaining fission gases), and failed DTF particles (i.e., DTF particles with a breached pyrocarbon layer) were expected to behave like TRISO particles with failed TRISO coatings (releasing both Cs and fission gases). DTF fuel kernels were coated only with a thin (20-μm-thick) pyrocarbon layer that was intentionally fabricated with high anisotropy so that it would fail during the irradiation (Collin 2015a; Hunn and Miller 2009; and Kercher et al. 2011), resulting in 20 exposed fuel kernels per compact. As shown on the right in Figure 1, the DTF particles (highlighted in red) were aligned roughly along the compact radial centerline.

The white particles in Figure 1 are the driver particles. AGR-3/4 driver particle fuel kernels were fully TRISO-coated with buffer, inner pyrolytic carbon (IPyC), SiC, and outer pyrolytic carbon (OPyC) layers, with characteristics similar to the "baseline" variant from the AGR-1 experiment (Collin 2015b; Hunn and Lowden 2007). Both the AGR-3/4 driver and DTF fuel particles contained fuel kernels (~350 μm in diameter) composed of a heterogenous mixture of uranium carbide and uranium oxide uranium oxycarbide (often abbreviated as UCO) that were manufactured by BWX Technologies Nuclear

Operations Group (Lynchburg, VA). The U-235 enrichment was 19.7 wt%. The DTF pyrocarbon coating and the driver fuel TRISO coatings were applied to the kernels at Oak Ridge National Laboratory. The driver particle and DTF particle properties are summarized in Collin (2015a). Complete kernel and particle characterization and fabrication data are compiled in several prior reports (Kercher and Hunn 2006; Hunn and Lowden 2007; Hunn and Miller 2009; Kercher et al., 2011). The average dimensions of the driver fuel particles and DTF particles are summarized in Table 1.

AGR-3/4 driver and DTF particles were over-coated with a precursor to the graphitic matrix material and formed into cylindrical fuel compacts at Oak Ridge National Laboratory. The compact graphitic matrix material was composed of multiple types of graphite and a carbonized phenolic resin. The compacts were nominally 12.3 mm in diameter and 12.5 mm long (in contrast to the AGR-1 and AGR-2 compacts, which were approximately 12.3 mm in diameter and 25 mm long). The AGR-3/4 fuel compact properties are summarized in the AGR-3/4 Final As-Run Report (Collin 2015a). Detailed characterization data on the as-fabricated compacts were compiled in Hunn, Trammel, and Montgomery (2011).

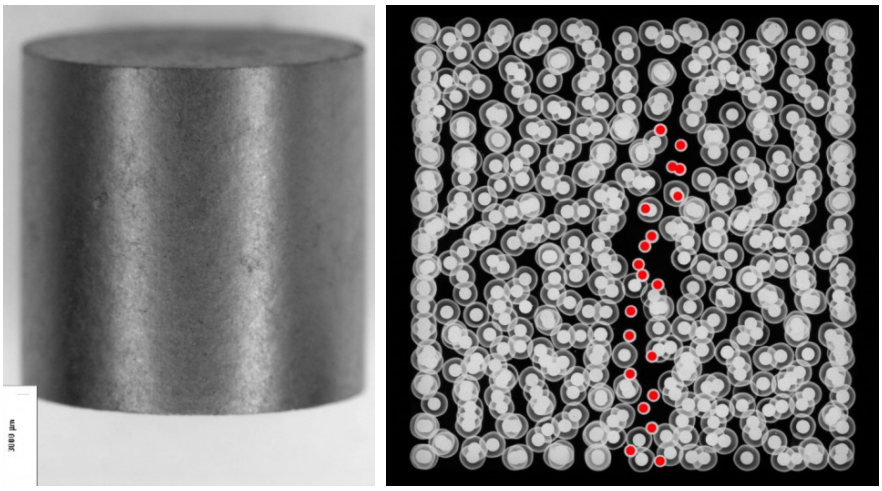

Figure 1. (Left) AGR-3/4 fuel compact. (Right) X-radiograph of a 2.5-mm-thick section taken from the center of an AGR-3/4 compact (Hunn, Trammell, and Montgomery 2011). The DTF particles are highlighted by red dots in the X-ray image.

Table 1. As-fabricated particle dimensions and standard deviations, from Table A-2 in Collin (2015a).

DTF Particle Properties	
Kernel diameter (µm)	357.3 ± 10.5
DTF pyrocarbon thickness (µm)	20.0 ± 9
DTF particle overall diameter (µm)	400.0 ± 9.2
Driver particle properties	
Kernel diameter (µm)	357.3 ± 10.5
Buffer thickness (µm)	109.7 ± 7.7
IPyC thickness (µm)	40.4 ± 2.3
SiC thickness (µm)	33.5 ± 1.1
OPyC thickness (µm)	41.3 ± 2.1
Driver particle overall diameter (µm)	818.9 ± 14.2

1.2. Irradiation and In-Pile DTF Failures

The AGR-3/4 experiment was irradiated in the Northeast Flux Trap at ATR for 369 effective full-power days (Collin et al. 2018). The AGR-3/4 irradiation test train consisted of 12 separate capsules, each with four fuel compacts. In each capsule, the four compacts were stacked within concentric rings of graphitic matrix material (using the A3-27 formulation) and/or nuclear-grade graphite (IG-110 and PCEA) (Collin et al. 2018). The capsules and compacts were numbered from bottom to top. Thus, Capsule 1 was at the bottom and Capsule 12 was at the top. The compact naming convention begins with the capsule number and then denotes the level of the compact within its respective capsule. For example, Compact 10-2 was the second compact from the bottom of Capsule 10. Online fission gas monitoring was used for each capsule during the AGR-3/4 irradiation in ATR (Collin et al. 2018).

Fission gas measurements were used to estimate the number of DTF particles to fail in-pile (with broken pyrocarbon layers) in each of the 12 AGR-3/4 irradiation capsules (Collin et al. 2018). Given the similarity to AGR-1 fuel, and based on experience from AGR-1, it was very unlikely that any AGR-3/4 driver particles failed during the irradiation. Thus, all estimated in-pile particle failures were assumed to be DTF failures. These estimates suggest that all 20 DTF particles had failed in all four compacts from Capsules 3 and 8. It is therefore assumed that Compacts 3-2 and 8-2 had no intact DTF particles at the start of the FACS heating tests.

Estimates from the in-pile fission gas measurements suggest that 36–75 DTF particle failures occurred in Capsule 10 (Collin et al. 2018). If each Capsule 10 compact had the same number of DTF failures, then each compact might have between 9 and 19 failed DTF particles at the start of a given heating test. There is no evidence to suggest that each compact would have had the same number of failures. It is also possible that all the DTF particles failed but that the fission gas monitoring was unable to resolve near-simultaneous failures of multiple particles.

One compact from each of AGR-3/4 Capsules 5, 7, and 12 has undergone compact cross-sectional analysis via sectioning, grinding, polishing, and optical microscopy (Stempien and Schulthess 2020). Of the 29 DTF particles that were found among the three compacts, no intact pyrocarbon layers were observed (Stempien and Schulthess 2020). Taking the compact ceramography and fission gas estimates into consideration, it was assumed that no intact DTF particles were present in Compacts 10-4 and 10-2 at the start of the FACS heating tests.

2. SAMPLE SELECTION, EXPERIMENTAL PROCESSES, AND DATA PROCESSING

2.1. Sample Selection

Table 2 lists the four AGR-3/4 compacts that underwent post-irradiation FACS testing, along with the selected irradiation properties and FACS test temperatures. Burnups are given in units of fissions per initial-metal-atom (FIMA), and temperatures are given as time-average (TA) and time-average volume-average (TAVA) values. Compacts 3-2, 10-2, and 10-4 have similar end-of-irradiation (EOI) burnups and TAVA temperatures, so testing them at different temperatures in FACS enables a comparison of fission product releases as a function of test temperature. Compact 8-2 had a higher irradiation temperature and higher burnup than Compact 10-4, so testing these two compacts at the same 1400°C temperature enabled exploration of how irradiation conditions affect fission product release.

It should be stated that the irradiation temperature-vs.-time histories that produced these averages may vary among the compacts. For instance, Capsule 3 had a steady volume-average fuel temperature of ~1200°C throughout the irradiation, but the Capsule 8 temperatures were less consistent, starting a little above 1200°C, dropping to ~1100°C at the mid-point of the ATR irradiation, and then reaching as high as 1350°C toward the end. Additionally, Compact 10-4 was at the top of the stack of four compacts in Capsule 10 and while its TAVA temperature was similar to the others, it had a TA minimum temperature

about 100°C lower than the other compacts discussed here. These time variations may affect the interpretation of the results.

Preliminary results from the FACS tests of Compacts 3-2, 10-2, and 10-4 were reported at a conference in 2018 (Stempien et al. 2018a). A subsequent test of Compact 8-2 was conducted in the FACS furnace at 1400°C, but it was not completed in time for inclusion in the aforementioned 2018 conference paper. Five additional AGR-3/4 compacts were reirradiated in the Neutron Radiography (NRAD) reactor prior to FACS testing at temperatures of 1000–1600°C. Preliminary results were reported for three of the five reirradiation-FACS tests in 2021 (Stempien et al. 2021b). A future report will cover the complete results for all five of those reirradiation-FACS tests.

Table 2. Compact irradiation histories and FACS test temperatures. The irradiation properties were taken from Sterbentz (2015) and Hawkes (2016). The compacts were heated in their as-irradiated condition (i.e., without reirradiation).

Compact	Burnup (% FIMA)	Neutron Fluence (10^{25} n/m^2, E>0.18 MeV)	TAVA Temperature (°C)	TA Minimum Temperature (°C)	TA Peak Temperature (°C)	FACS Temp. (°C)
3-2	12.49	4.17	1196	1154	1240	1600/ 1700
8-2	14.58	5.11	1213	1171	1257	1400
10-2	11.96	4.01	1190	1179	1249	1200
10-4	11.43	3.75	1168	1079	1231	1400

2.2. FACS Tests

2.2.1. Furnace Operation

Each of the four compacts listed in Table 2 was heated separately in the FACS furnace at INL. A schematic of the FACS furnace is given in Figure 2. A tantalum sample holder held the compact in the tantalum flow tube. A helium sweep gas passed through the apparatus at a total flow rate of 1 L/min. A water-cooled cold finger held condensation plates to collect condensable fission products. The condensation plates were exchanged at various points during the test. The plates were then gamma counted and leached for fission products. A fission gas monitoring system (FGMS) collected and counted Kr-85 throughout the test.

Each test began with a 2-h heat-up from ambient temperature to 300°C, and a 2-hr hold at 300°C to drive off any moisture from the compacts. Next, the furnace temperature was increased to the test temperature in 2 hours. The test temperature was held constant for at least 300 hours. Multiple condensation plates were exchanged during the hold at the test temperature, and a plate exchange was made 30 minutes before and after the temperature was changed during the heat-up and cooldown phases. Additional information on the FACS furnace is available in Demkowicz et al. (2012).

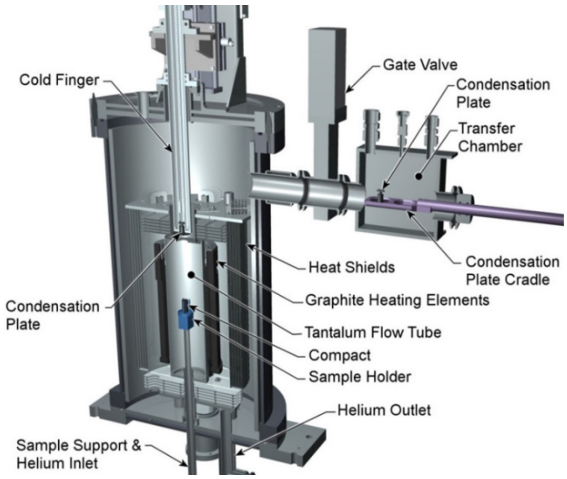

Figure 2. FACS furnace schematic (Demkowicz et al. 2012).

2.2.2. Post-test Analysis

The activities of gamma-emitting fission products and beta-emitting Sr-90 on each condensation plate were measured and decay-corrected back to the AGR-3/4 end of irradiation (EOI) plus one day (EOI+1). The AGR-3/4 irradiation ended on April 12, 2014, at 5:00 AM Mountain Time. The decay-corrected activities were then divided by the predetermined FACS furnace condensation plate collection efficiencies (summarized in Table 3). Though there are no collection efficiencies for Ce/Pr-144, trace amounts are occasionally detected. In such cases, a collection efficiency of 1 is used. Fission gases (i.e., Kr-85) detected in the FGMS cold traps were also decay-corrected to EOI+1. To give the compact fraction released from the fuel during the FACS tests, the measured decay- and efficiency-corrected activities on the condensation plates and the decay-corrected activities of Kr-85 in the FGMS were divided by the compact fission product inventory predictions based on physics calculations reported in Sterbentz (2015).

The majority of the Ag-110m in the compacts from Capsules 3, 8, and 10 was released during irradiation, prior to the heating test (Stempien et al. 2018b). Taking the inventory of Ag-110m measured in each compact via post-irradiation gamma scanning (Harp, Stempien, and Demkowicz 2021) and dividing that by the inventory calculated via physics simulations (Sterbentz 2015) gives a rough estimate that the Ag-110m in-pile releases were as follows: Compact 3-2, 93%; Compact 8-2, 86%; Compact 10-2, 80%; and Compact 10-4, 95%. Thus, the Ag-110m inventories in the compacts were already low at the start of the heating tests.

Table 3. FACS furnace condensation plate fission product collection efficiencies.

	Collection Efficiency at 1600°C[a]	**Collection Efficiency at 1400°C[b]**	**Collection Efficiency at 1200°C[b]**
Ag-110m	0.503	N/A[c]	N/A[c]
Cs-134	0.661	0.397	0.427
Eu-154	0.286	0.035[d]	0.017
Sb-125	0.574[e]	0.359	0.297
Sr-90	0.333	N/A[c]	N/A[c]

a. See (Demkowicz et al. 2012) and (Demkowicz et al. 2015b).
b. These efficiencies were determined from FACS tests of cracked particles from AGR-2 Compacts 5-4-2 and 2-2-1.
c. Efficiencies not available. For 1400°C and 1200°C tests, use the collection efficiencies at 1600°C for Ag-110m and Sr-90.
d. This value was determined by averaging the collection efficiency at 1600°C and 1200°C.
e. Determined from a FACS test of loose kernels from AGR-2 Compact 6-4-1. There is no information on the repeatability of this value.

3. RESULTS

The results for selected isotopes (i.e., Ag-110m, Cs-134, Eu-154, Kr 85, Sb-125, and Sr-90) are given here. Cs-137 and Eu-155 were also measured, but are not plotted here. The Cs-137 and Cs-134 measurements were generally in good agreement, but trace contamination of the longer-lived Cs-137 in the hot cells often biased the Cs-137 readings higher than the Cs-134 measurements. The Eu-155 and Eu-154 measurements generally agreed within 15%; however, in comparison to Eu-155, Eu-154 has higher-energy gamma rays that were more consistently measured (with lower error). Thus, only Eu-154 is plotted to represent europium. In Figure 3, the dashed line labeled "Particle" represents the compact fraction (5.21E-4) equivalent to a single particle inventory of fission products, and the dashed line labeled "DTF Particles" represents the compact fraction equivalent to 20 particles. The FACS furnace temperature measured at the thermocouple in the sample holder is plotted in the summary figures.

3.1. 1600/1700°C Test of Compact 3-2

Figure 3 shows the temperature program for this test and summarizes the measured compact fractional releases as a function of test time. Compact 3-2 was held at 1600°C from 6 hours until 335.5 hours. During this period, 0.31 particle equivalents (a compact fraction of 1.62E-4) of Kr-85 were detected in the FGMS traps. To see if significantly more Kr-85 would be released at a higher temperature, the temperature was raised from 1600 to 1700°C over the course of one hour, and this new temperature was maintained from a total elapsed time of 336.5 hours until 383.7 hours. An additional 5% of one particle worth of Kr-85 was released during the 1700°C hold, indicating that only about 0.37 particle equivalents of Kr-85 remained in this compact after the irradiation in ATR.

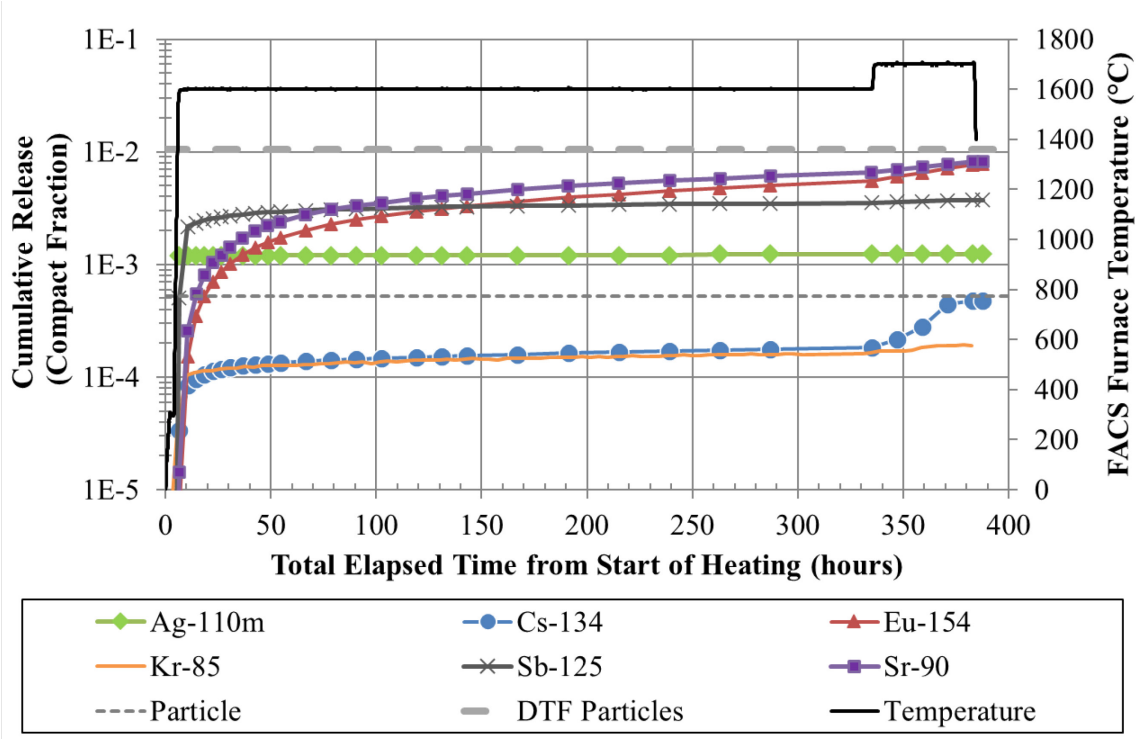

Figure 3. Summary of select fission product releases from the Compact 3-2 1600/1700°C test.

Table 4 summarizes the total fractional releases that occurred during the 1600°C and 1700°C holds. Of the 31 condensation plates exchanged during the test, only two had measurable quantities of Ag-110m: plate #2 (inserted in the FACS furnace 30 minutes before the ramp from 300°C and removed 30 minutes

after reaching 1600°C) and plate #24 (inserted at 239 hours and removed 24 hours later at a constant 1600°C).

Cesium-134 was measured on all condensation plates. From the start of the test and up to the beginning of the ramp from 1600°C to 1700°C, a fraction of 1.83E-4 (0.346 particle equivalents) was released. During the hold at 1700°C, an additional fraction of 2.98E-4 (0.571 particle inventories) was released. This suggests that most of the Cs-134 in the DTF particles had been released in-pile during the irradiation in ATR, and the as-irradiated RDLBL of compacts with similar EOI burnups and TAVA temperatures supports this assertion. The as-irradiated RDLBL of Compact 3-3 faced some accidental particle damage during the exams, making it difficult to determine the true post-irradiation inventory of Cs-134 in the compact outside of the TRISO particle SiC layers (Stempien and Cai 2024a). However, as-irradiated RDLBL of Compacts 8-3 (Stempien and Cai 2024a) and 8-4 (Helmreich et al. 2021) measured 1.5 and 0.5 particle equivalents, respectively, of Cs-134 remaining in the compacts in the matrix, OPyC coatings, and DTF particles. Section 4.2 contains additional discussion of the cesium behavior in this and other compacts.

For Eu-154 and Sr-90, the release fraction-vs.-time behaviors and total fractional releases were similar, totaling about 15 and 16 particle equivalents, respectively. Given the 20 DTF particles in the compact and the 15 or 16 particle equivalents of Eu-154 and Sr-90 measured, this could be dominated by the Eu and Sr produced in the DTF particles. It also may be that a small amount of Eu and Sr released through intact TRISO coatings in-pile were contributing to the observed release of Eu and Sr in the FACS test.

The fractional release of Kr-85 was similar to that of Cs-134 during the 1600°C period; however, unlike Cs-134, very little additional Kr-85 was released after increasing the test temperature to 1700°C. More than 60% of the Sb-125 release occurred in the first four condensation plates (from the start of heating to 10.5 hours at 1600°C), followed by relatively steady release throughout the remainder of the time at 1600°C.

There were increases in the Kr-85, Cs-134, Eu-154, Sb-125, and Sr-90 release rates upon increasing the test temperature to 1700°C (see Figure 4). It is important to note that in Figure 4, the final data point at ~385 h is not representative of steady-state behavior because this plate was installed on the FACS furnace's cold finger about 30 minutes before the ramp down from 1700°C was initiated. The Kr-85 rate increased during and shortly after the ramp to 1700°C was complete. For the remaining ~24 hours at 1700°C, it then decreased to a rate similar to the first ~150 hours at 1600°C. (See Section 4.5 for a depiction of the Kr-85 release rates.) The Cs and Sb release rates initially increased upon the temperature reaching 1700°C. Then, they began to decrease. This may indicate that the higher temperature promoted transport of Cs and Sb from wherever they resided in the compact outside of the intact TRISO particles (e.g., DTF kernels and compact graphitic matrix). Then, as that reservoir was depleted, the rate began to slow. The Eu and Sr behavior demonstrated an increase in the release rate that was steady as long as 1700°C was maintained. This is likely evidence of greater quantities of Eu and Sr than Cs and Sb remaining outside of intact TRISO coatings in the compact (e.g., in DTF kernels or in the compact matrix).

Table 4. Fission product releases from Compact 3-2 during the FACS test. The compact fraction is given with no parentheses, and particle equivalents are given in parentheses.

Compact 3-2	Release at 1600°C	Released at 1700°C	Total
Ag-110m	1.24E-3 (2.38)	None detected	1.24E-3 (2.38)
Ce-144	None detected	None detected	None detected
Cs-134	1.83E-4 (0.35)	2.98E-4 (0.57)	4.81E-4 (0.92)
Eu-154	5.55E-3 (10.64)	2.22E-3 (4.25)	7.76E-3 (14.89)
Kr-85	1.64E-4 (0.314)	2.80E-5 (0.054)	1.92E-4 (0.368)
Sb-125	3.52E-3 (6.75)	2.09E-4 (0.40)	3.73E-3 (7.15)
Sr-90	6.52E-3 (12.50)	1.70E-3 (3.25)	8.22E-3 (15.76)

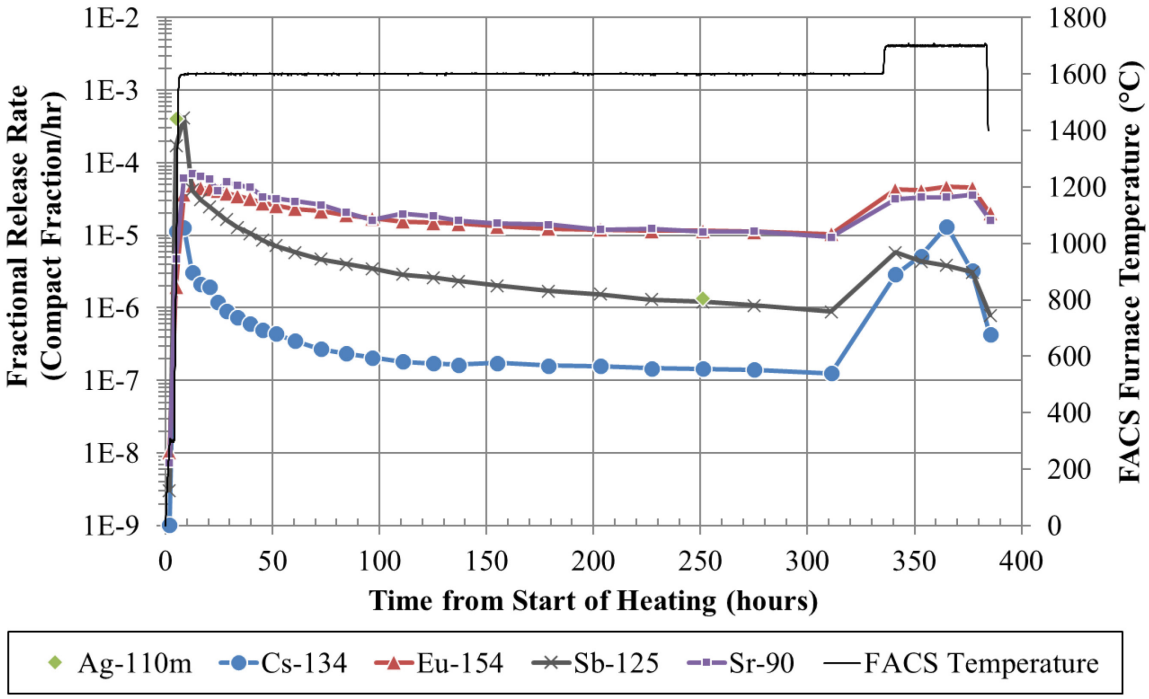

Figure 4. Summary of condensable fission product release rates from the Compact 3-2 1600/1700°C test.

3.2. 1400°C Test of Compact 8-2

Figure 5 shows the cumulative fission product release as well as the temperature profile as a function of test time for Compact 8-2. There will be uncertainty in these data related to the FACS collection efficiencies, which do not exist for Sr-90 and Ag-110m at 1400°C (see Table 3). The total releases from the compact during the test are summarized in Table 5. About 90% of Ag-110m release from this test was measured on the second condensation plate. This plate was inserted 30 minutes prior to the ramp from 300 to 1400°C, and it was removed 15 minutes after the ramp to 1400°C was complete. This behavior is related to the previously observed phenomenon in which the Ag-110m release rate peaks at intermediate temperatures ranging from about 1100–1300°C (Hunn et al. 2015a). Ag-110m was the only nuclide to

have total releases similar to the fraction of DTF particles in the compact (~1%). The Sb-125 release totaled 2.5 particle equivalents. The rest of the nuclides (i.e., Kr-85, Cs-134, Eu-154, and Sr-90) were released in totals less than a single particle equivalent (<5E-3 compact fraction). Trace amounts of Ce-144 were detected on three of the 19 condensation plates (totaling 7.80E-4 particle equivalents), indicating that nuclide is well retained despite the presence of 20 DTF particles in the compact.

The amounts of Eu and Sr measured from this test are influenced by the FACS condensation plate efficiencies. An efficiency for Eu could not be determined from the separate loose particle tests conducted at 1400°C, so one was estimated by averaging the 1600°C collection efficiency with that determined from a 1200°C test of loose particles. This gives an Eu collection efficiency 10x lower at 1400°C than at 1600°C. Because it does not have gamma-ray emissions, no collection efficiencies could be determined for Sr-90 via the loose-particle tests, and the only available Sr-90 collection efficiency is for 1600°C. If it were assumed that the Eu and Sr collection efficiencies should be similar, one could estimate a Sr collection efficiency by using one from Eu. If that were done, the Sr and Eu values in Figure 5and Table 5 would be very similar. The shape of the Eu and Sr release- vs.-time is typical for these nuclides.

Figure 6 summarizes the FACS temperature program and the release rates of condensable fission products from the 1400°C test of Compact 8-2. (See Section 4.5 for a depiction of the Kr-85 release rates.) It is important to note that in Figure 6, the final data point at ~310 h is not representative of steady-state behavior because this plate was installed on the FACS furnace's cold finger about 30 minutes before the ramp down from 1400°C was initiated. As stated earlier, the majority of the Ag-110m detected from this test was released at the beginning of the test, before the temperature reached 1400°C. The rate dropped dramatically on the next condensation plate in the sequence. The Ag-110m rate slowly decreased as the test progressed and the Ag-110m inventory outside the intact SiC coatings was being depleted, with a slight increase for the final plate used in the furnace primarily during the cooldown phase, where it would have passed through the intermediate temperature region (1100−1300°C) where Ag release from intact TRISO particles is most rapid.

The Cs release rate was highest early on in the Compact 8-2 test, and it decreased with time at the isothermal hold. The Eu-154 and Sr-90 release rates increased slightly but steadily as the Compact 8-2 1400°C test progressed. This might be due to the more gradual mobilization of Eu and Sr at 1400°C (which will eventually subside as the source is depleted) in comparison to the rapid initial release at 1600°C in the other test. The Sb-125 release rates vs. time somewhat mimicked that of Ag-110m, except that they were slower than the Ag-110m rates.

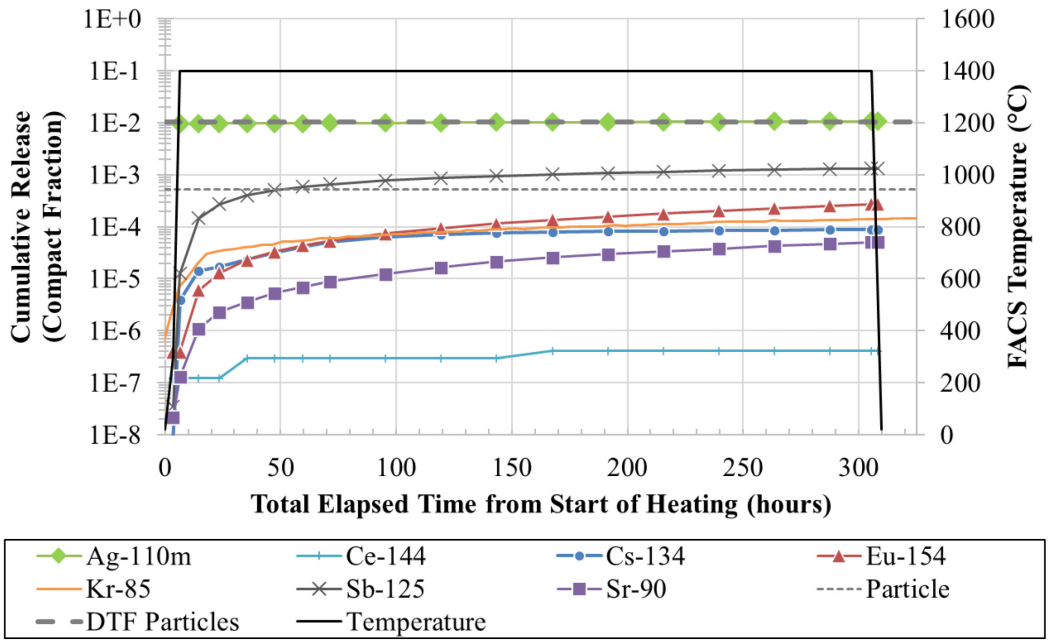

Figure 5. Summary of select fission product releases from the Compact 8-2 1400°C test.

Table 5. Fission product releases from Compact 8-2 during the FACS test.

Compact 8-2 Total Release at 1400°C		
	Compact Fraction	Particle Equivalents
Ag-110m	1.07E-02	20.6
Ce-144	4.07E-07	7.8E-4
Cs-134	8.88E-05	0.17
Eu-154	2.73E-04	0.52
Kr-85	1.43E-04	0.27
Sb-125	1.32E-03	2.54
Sr-90	5.07E-05	0.10

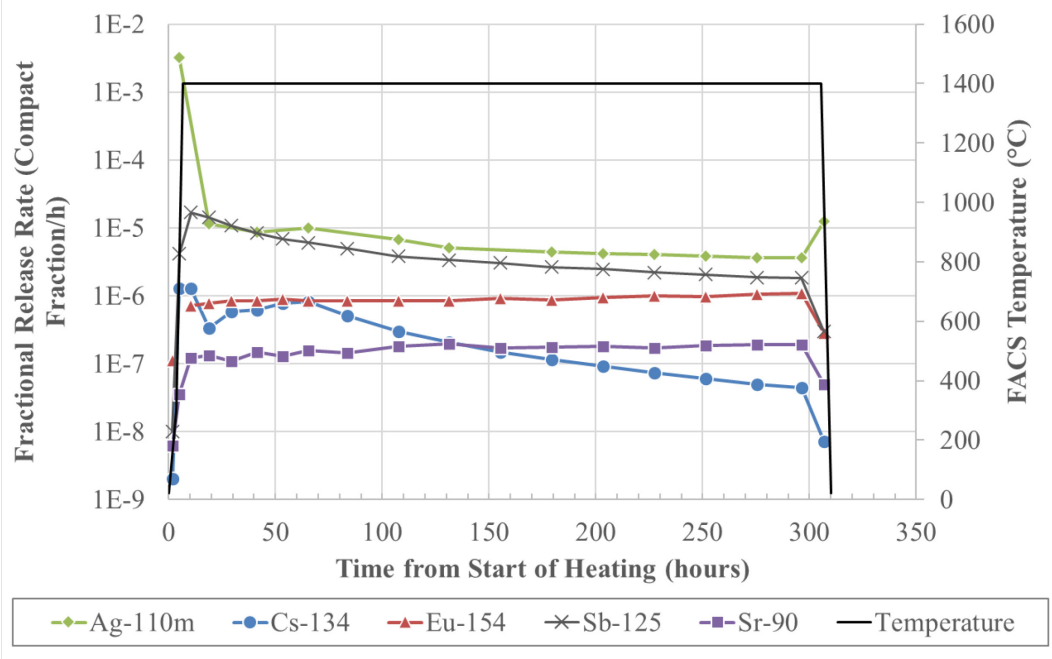

Figure 6. Summary of condensable fission product release rates from the Compact 8-2 1400°C test.

3.3. 1400°C Test of Compact 10-4

Compact 10-4 was held at 1400°C for 300 hours, and 22 condensation plates were exchanged during this test. Figure 7 summarizes the compact fractional fission product releases as a function of test time. Table 6 summarizes the total releases for selected isotopes. The total fraction of detected Ag-110m release was 4.40E-3, which is equivalent to 8.44 particle inventories. More than half of all the measured Ag-110m released was on the second condensation plate, very similar to what was observed in the 1400°C test of Compact 8-2. Any Ce-144 that may have been released was below the detectable limit. The Eu-154 and Sr 90 releases and release-vs.-time behaviors were similar. The Kr-85 and Cs-134 release fractions were also similar. The initial release of Sb-125 was lower than that of Ag-110m until about 100 hours after the start of the heating, after which the Sb-125 release behavior was similar to that of Ag-110m.

The same uncertainties in FACS furnace collection efficiencies that impacted the results from the 1400°C test of Compact 8-2 impact this test as well. Figure 8 shows the time-dependent release rates, which are very similar to those from the Compact 8-2 1400°C test in terms of both their values and their time variation. The biggest difference is that the initial peak in the Cs-134 release rate from Compact 10-4 in the first 9 hours of the test that was not present in the test of Compact 8-2. It is important to note that in Figure 8, the final data point at ~310 h is not representative of steady-state behavior because this plate was installed on the FACS furnace's cold finger about 30 minutes before the ramp down from 1400°C was initiated.

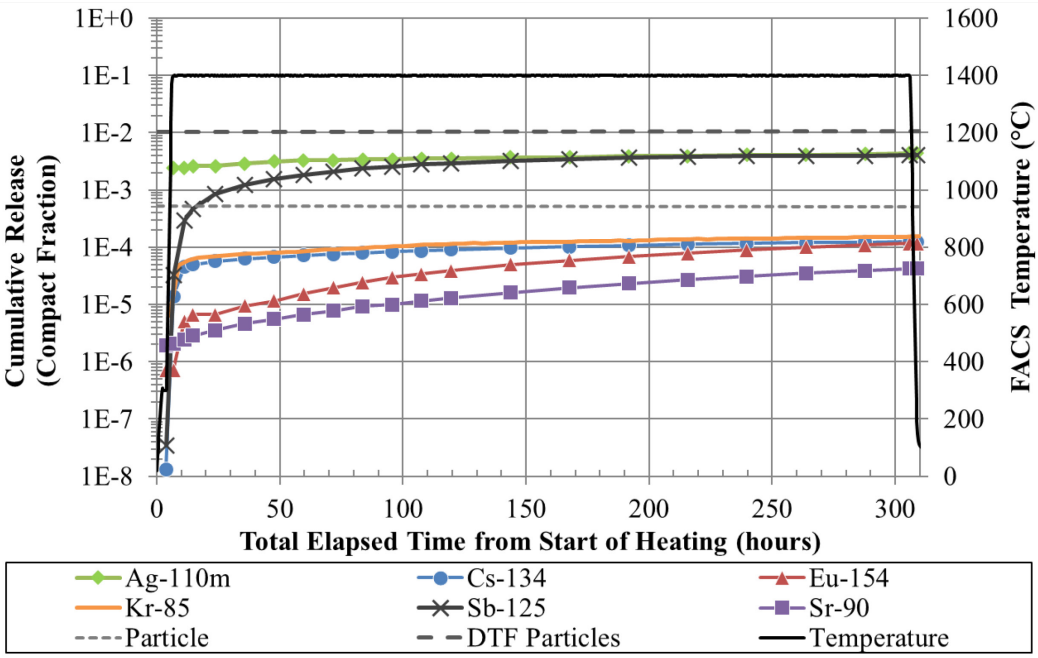

Figure 7. Summary of select fission product releases from the Compact 10-4 1400°C test.

Table 6. Fission product releases from Compact 10-4 during its 1400°C FACS test.

	Compact Fraction	Particle Equivalents
Ag-110m	4.40E-3	8.44
Ce-144	<9.83E-6	<1.89E-2
Cs-134	1.25E-4	0.24
Eu-154	1.16E-4	0.22
Kr-85	1.53E-4	0.29
Sb-125	4.03E-3	7.72
Sr-90	4.22E-5	0.08

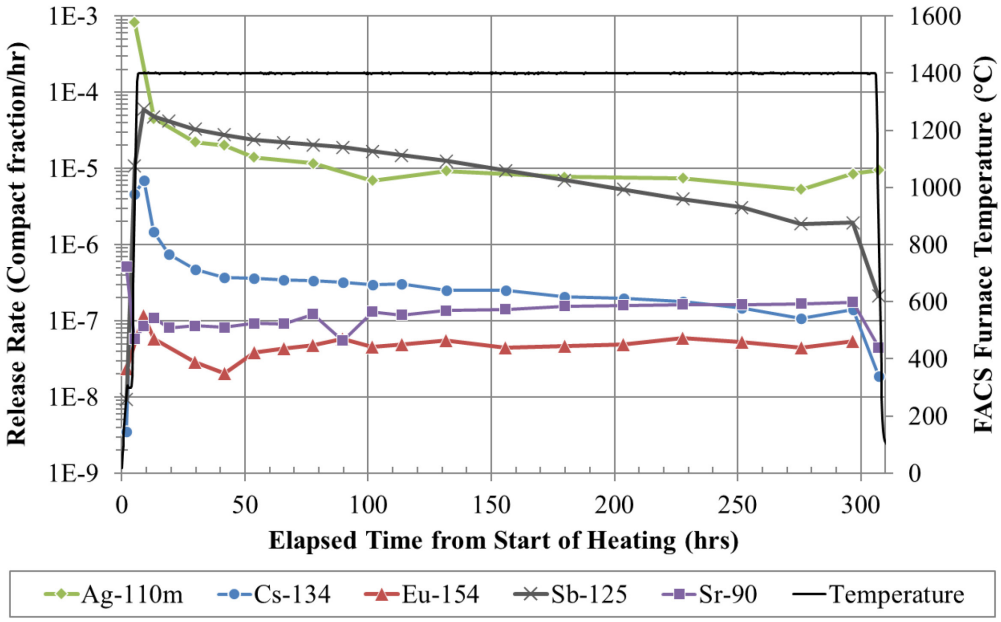

Figure 8. Summary of condensable fission product release rates from the Compact 10-4 1400°C test.

3.4. 1200°C Test of Compact 10-2

Compact 10-2 was held at 1200°C for 300 hours, and 19 condensation plates were exchanged during this test. Figure 9 summarizes the compact fractional fission product releases as a function of test time, Table 7 summarizes the total releases for selected isotopes after completion of the test, and Figure 10 gives the time-dependent release rates for the condensable fission products. Once again, it is important to note that in Figure 10, the final data point at ~310 h is not representative of steady-state behavior because this plate was installed on the FACS furnace's cold finger about 30 minutes before the ramp down from 1200°C was initiated. The TAVA irradiation temperature for Compact 10-2 was 1190°C; therefore, this 1200°C test provides information for comparison to the hotter tests of Compacts 3-2, 8-2, and 10-4, as well as information on the release rates during the Compact 10-2 irradiation in ATR. Ag-110m was measured on 18 of the 19 plates and was the only isotope released in quantities exceeding a single particle equivalent. In fact, the Ag-110m release fraction exceeded the amount available from the DTF particles, which means that release of Ag-110m from intact TRISO particles contributed to the Ag measured here. Eu-154 was measured on only four plates. Sr-90 was measured on all plates, but the total Eu and Sr releases were similar. The Kr-85, Cs-134, and Sb-125 fractional releases and release-vs.-time behaviors were similar. The total releases from this test were considerably less than in the 1400°C+ tests.

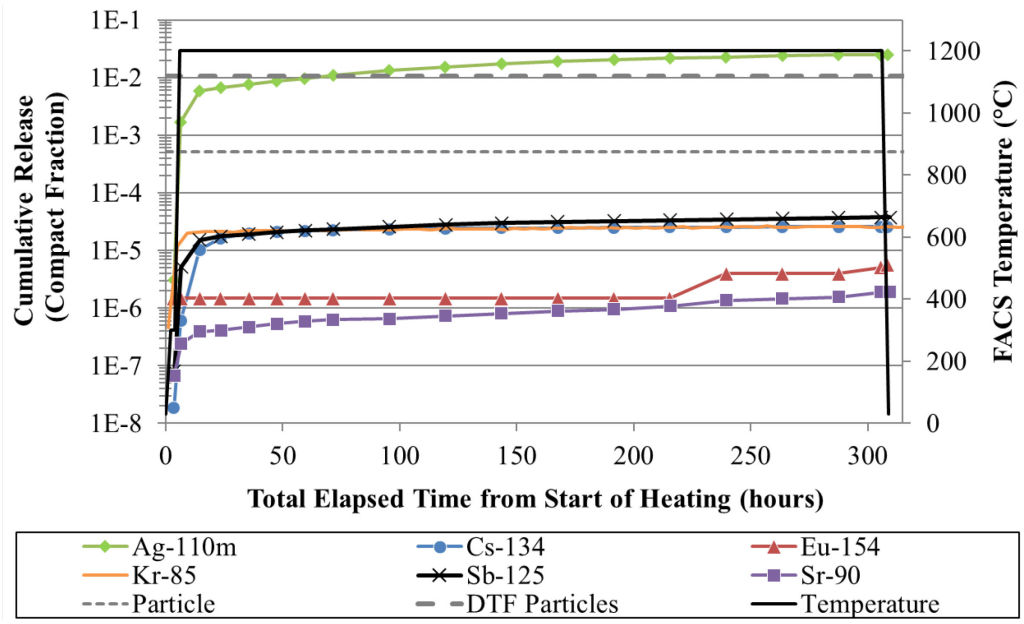

Figure 9. Summary of select fission product releases from the Compact 10-2 1200°C test.

Table 7. Fission product releases from Compact 10-2 during its 1200°C FACS test.

	Compact Fraction	Particle Equivalents
Ag-110m	2.51E-2	48.1
Ce-144	<2.06E-6	<3.95E-3
Cs-134	2.59E-5	4.96E-2
Eu-154	5.55E-6	1.06E-2
Kr-85	2.65E-5	5.08E-2
Sb-125	3.73E-5	7.16E-2
Sr-90	1.92E-6	3.67E-3

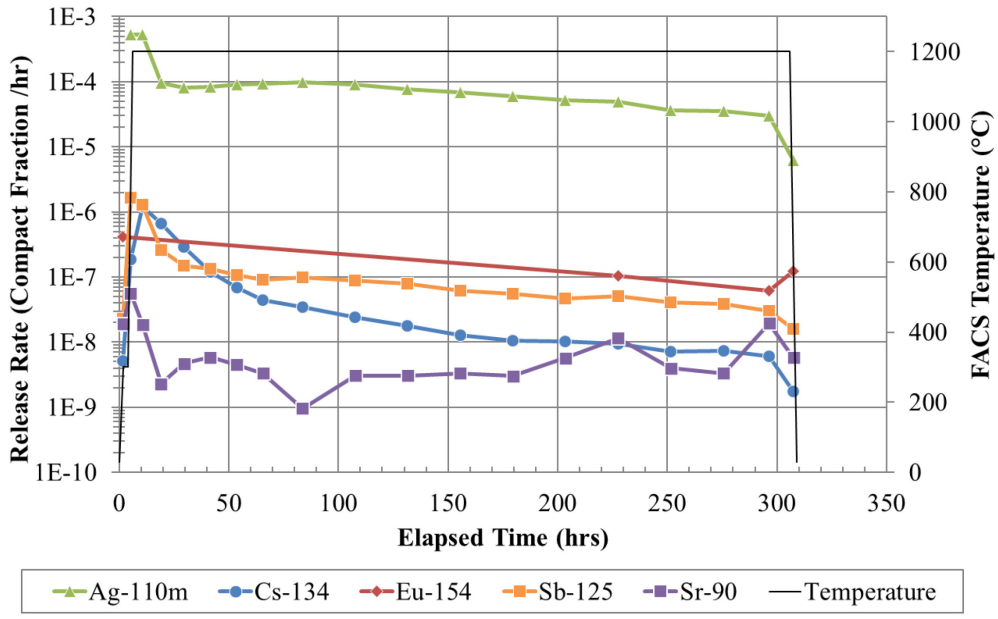

Figure 10. Summary of condensable fission product release rates from the Compact 10-2 1200°C test. Note that Eu-154 was only measured on four condensation plates.

4. DISCUSSION

This section compares the total quantities of Ag-110m, Cs-134, Eu-154, Sr-90, and Kr-85 released during these AGR-3/4 FACS tests, along with the rates of their release. The rates were determined via two methods. For the condensable fission products, the release rates (compact fraction/h) were computed by dividing the inventory on each individual condensation plate by the amount of time the plate was in the FACS furnace. In addition, average release rates for the condensable fission products were determined from the slope of a linear regression of cumulative release over the period of time at the isothermal hold where the coefficient of determination (R^2) was 0.9 or higher. Most often, the R^2 value was >0.95 in these regressions. Because Kr-85 was collected in a single cold trap, and there were point-to-point variations (within the statistical accuracy of the system) in the total Kr-85 detected in the traps as a function of time, the cumulative Kr-85 release vs. time was plotted, and linear fits were used to determine Kr-85 release rates for specific segments of each test. Comparisons to AGR-1 and AGR-2 will be made in some of the discussions and plots that follow. Those AGR-1 and AGR-2 data were previously compiled in several reports (Demkowicz et al. 2015a; Stempien et al. 2021a; Stempien, Cai, and Demkowicz 2023). Each of those reports lists other references with details of those examinations (if applicable).

4.1. Silver Behavior

Figure 11 shows the Ag-110m release fractions and release rates for each AGR-3/4 compact from each test. The temperature profiles for each test were plotted in Sections 3.1–3.4. Figure 12 and Figure 13 show the total Ag-110m released and the pseudo-steady-state release rates, respectively, in these AGR-3/4 tests as compared to post-irradiation tests of AGR-1 and AGR-2 compacts. In these plots, it is difficult to identify trends in the post-irradiation heating test results that are linked to the fuel EOI irradiation properties (burnup and TAVA temperature). Nevertheless, they provide a visual summary to aid in the comparison of AGR-1, AGR-2, and AGR-3/4, and techniques such as machine learning may be employed to attempt to deconvolute the data sets in Figure 12 and Figure 13.

Comparing the measured post-irradiation Ag-110m inventory (after the ATR irradiation but prior to FACS testing) to the calculated inventory from physics calculations gives an estimate that Compact 3-2 had retained roughly 7% of the Ag 110m predicted to have been produced in it during irradiation (Harp, Stempien, and Demkowicz 2021). This is deemed to be only an estimate of retention because of the measurement uncertainty in gamma scanning and potential biases in the physics calculations. Using the same method, it was estimated that Compacts 8-2, 10-4, and 10-2 had retained 14%, 5%, 20% of their Ag-110m after irradiation, respectively. Thus, each of the compacts was estimated to have released 80 to 95% of their Ag-110m in-pile before the FACS tests began.

Potential contributors to the total Ag-110m measured during the heating tests are inventories remaining in the compact matrix at EOI (this could be inventory that originated in the DTF particles or that diffused through intact TRISO-coated driver particles), in-furnace release from driver particles (i.e., release through intact TRISO coatings), and release from any small residual inventory remaining in the DTF kernels. However, it is not always possible to determine how much of the Ag-110m measured in the FACS furnace was from any of these potential sources.

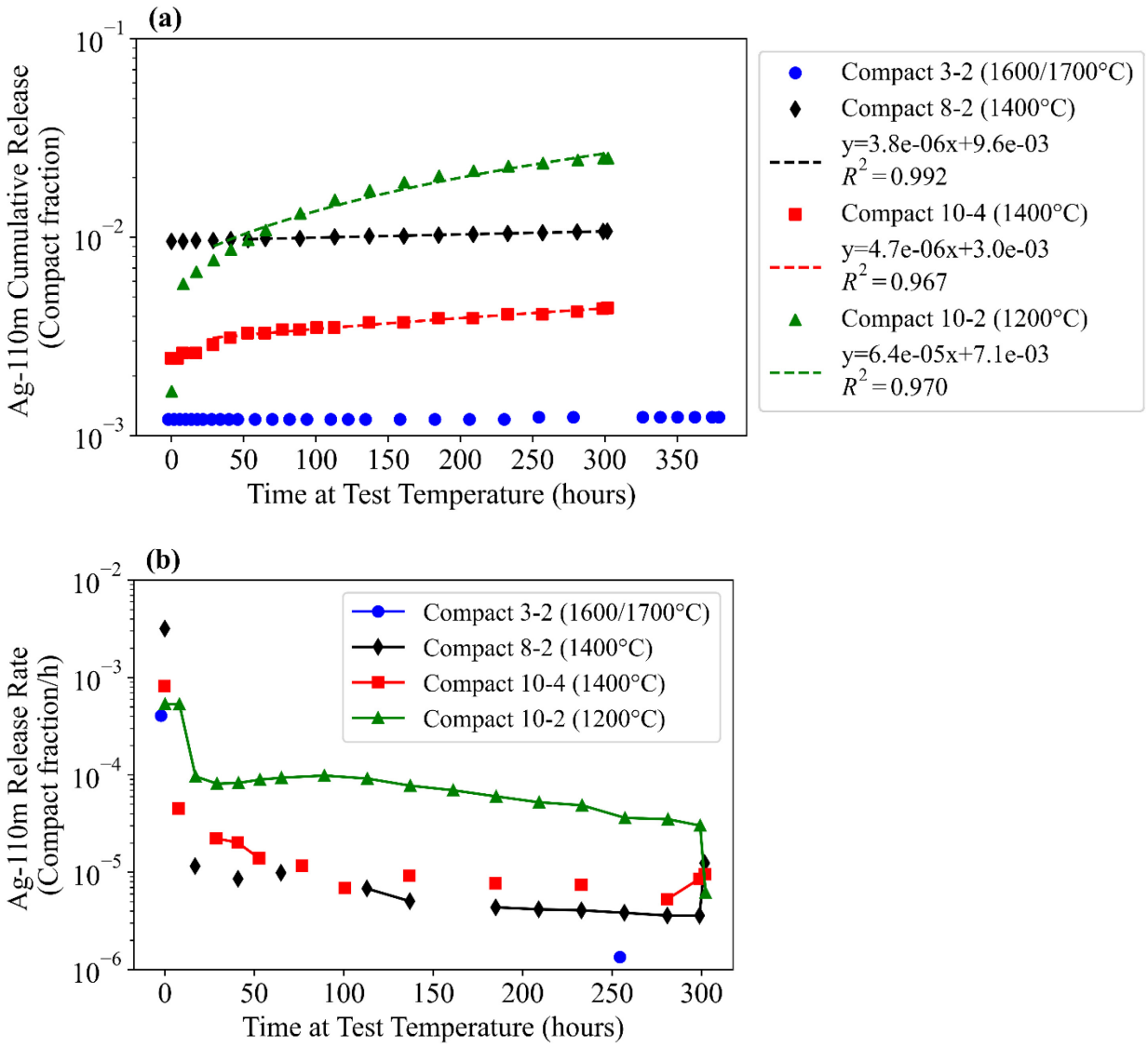

Figure 11. Ag-110m (a) release fractions and (b) release rates for the AGR-3/4 compacts.

In each test, the silver release rates were highest during the ramp to test temperature, and ranged from 4E-4 to 3.2E-2 compact fraction/h. After reaching the test temperature, release rates noticeably dropped and tended to decrease with time at the isothermal holds, presumably as the major sources of the Ag-110m were depleted. Prior heating tests of irradiated AGR-1 and AGR-2 fuel also showed that Ag release rates were highest in the initial stages of heating as Ag that was released to, and retained in, the compact matrix during irradiation was released upon heating (Demkowicz et al. 2015b, Morris et al. 2016).

After this early period, the AGR-3/4 Compact 3-2 rate at 1600°C decreased to 0, whereas the rates at 1400°C decreased to around 8E-6 compact fraction/h for Compact 10-4, and 4E-6 h^{-1} for Compact 8-2. These rates likely underestimate the true values because the only FACS condensation plate collection efficiency available for Ag-110m is for 1600°C, and the true efficiency at 1400°C is believed to be lower than that. Even so, 8E-6 h^{-1} exceeds the rates for most of the AGR-1 Compact 4-3-3 1600°C test and all but the very beginning of the AGR-1 Compact 6-4-1 test (Demkowicz et al. 2015b).

Notably, the Ag-110m release rate for most of the 1400°C test of AGR-3/4 Compact 10-4 (1E-5 h^{-1}) was higher than the silver release rate for AGR-1 Compact 4-2-2 at 1450°C by about a factor of 10 (Hunn

et al. 2015a). This higher rate for AGR-3/4 Compact 10-4 may be due to it being closer to the intermediate temperature range (1100−1300°C), where Ag release rates are most rapid. During that multi-temperature test of AGR-1 Compact 4-2-2 (Hunn et al. 2015a), the Ag-110m release rate increased from 1E-6 h^{-1} at 1450°C to 2E-5 h^{-1} at 1300°C, and the rate at 1150°C was 3.9E-5 compact fraction/hr.

The 1200°C test of AGR-3/4 Compact 10-2 clearly shows significantly more Ag-110m release (2.51E-2 fraction and 48.1 particle equivalents) than the three hotter tests at 1400°C and 1600°C+ because it was heated at a temperature in the middle of the range (1100−1300°C) where Ag-110m release is most rapid (Hunn et al. 2015a). The amount of Ag-110m release from Compact 10-2 was more than double what would be expected from the DTF particles alone, and this supports the hypothesis that intact driver particles dominated the total Ag-110m release during the AGR-3/4 Compact 10-2 heating test.

The 1400°C tests of Compacts 8-2 and 10-4 and the 1600/1700°C test of Compact 3-2 released notably less Ag-110m than the Compact 10-2 1200°C test. Relatively little Ag-110m was measured from the Compact 3-2 1600/1700°C FACS test. Compacts 8-2 and 10-4 had total Ag-110m releases in FACS that were about 9x and 4x higher, respectively, than the 1600/1700°C FACS test of Compact 3-2. This is despite the estimated Ag-110m inventories in Compacts 8-2 and 10-4 at the beginning of the FACS tests being both higher and lower (i.e., 2x and 0.7x), respectively, than in Compact 3-2 (Harp, Stempien, and Demkowicz 2021). This difference is in total release is attributed again to the higher Ag-110m release rates in and around the intermediate temperature range (1100−1300°C). This effect is also reflected in the Ag-110m release rates determined from these tests. Figure 11b shows that, on average, the rate at 1200°C was higher than the rates at 1400°C, which were higher than the rates determined from the only two condensation plates where Ag-110m was detected in the 1600/1700°C test of Compact 3-2.

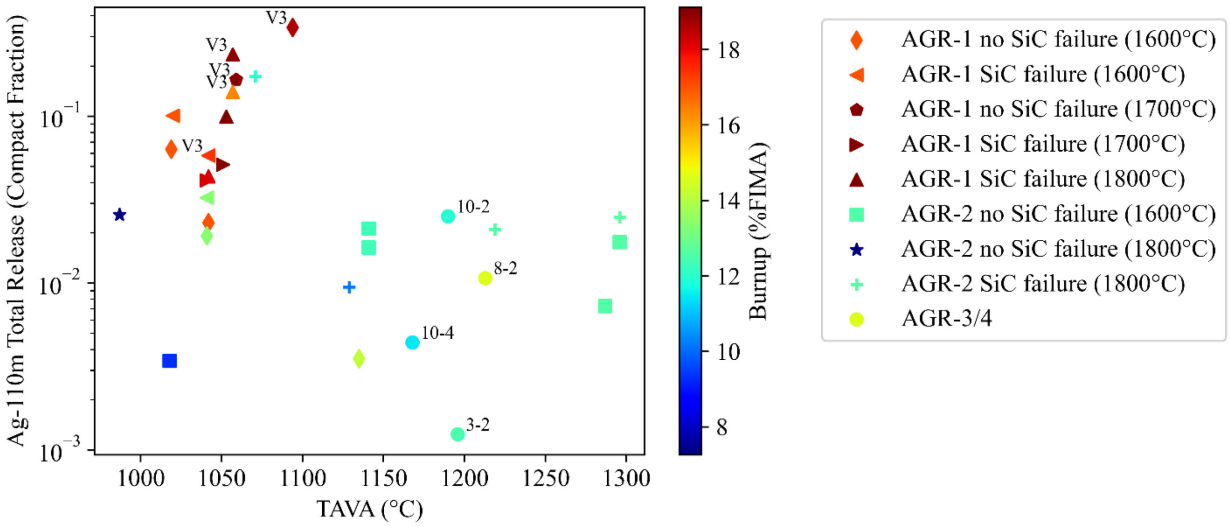

Figure 12. Total Ag-110m release during post-irradiation AGR-3/4 heating tests and AGR-1 and AGR-2 post-irradiation safety tests, as a function of compact TAVA temperature and burnup. The compact ID is labeled next to the four AGR-3/4 compacts in the plot. The legend also indicates whether the tested compacts experienced SiC failure.

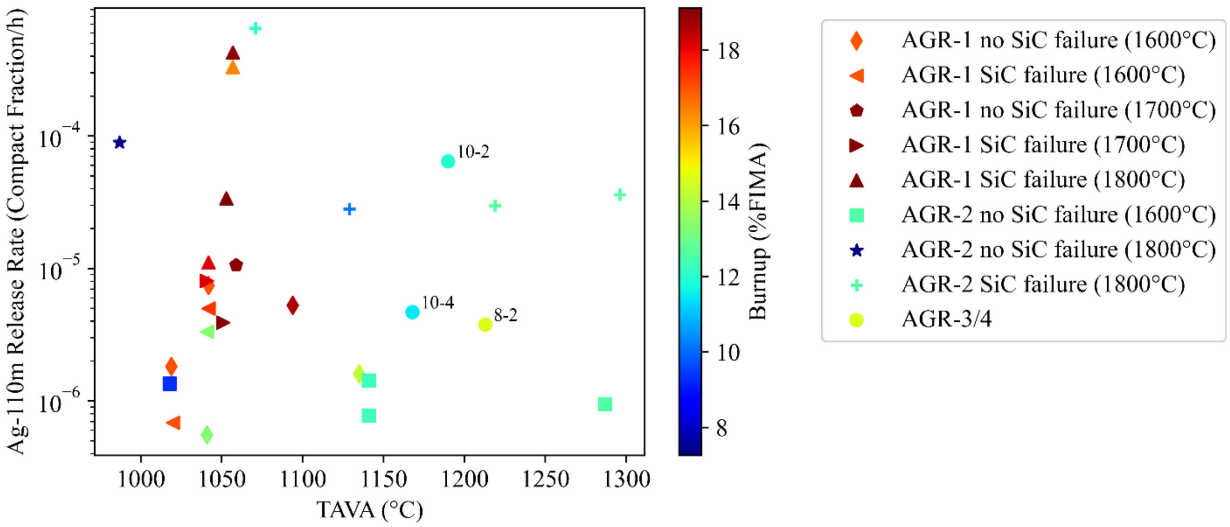

Figure 13. Average pseudo-steady-state release rates of Ag-110m from post-irradiation AGR-3/4 heating tests and post-irradiation AGR-1 and AGR-2 safety tests, as a function of compact TAVA temperature and burnup. The compact ID is labeled next to the four AGR-3/4 compacts in the plot. The legend also indicates whether the tested compacts had SiC failure.

4.2. Cesium

Figure 14 summarizes the cesium releases and release rates for AGR-3/4 Compacts 3-2, 8-2, 10-4, and 10-2. The total fraction of Cs-134 released from the 1600/1700°C Compact 3-2 test was 4.81E-4 (0.92 particle equivalents). Previous testing of AGR-1 fuel compacts demonstrated that Cs-134 fractional release from compacts with no exposed kernels was between approximately 2E-7 and 5E-6 after 300 h at 1600°C (Demkowicz et al. 2015b, Morris et al. 2016). The significantly higher release from the 1600°C portion of the AGR-3/4 Compact 3-2 test is due to Cs-134 from the DTF particles that remained in the compact after irradiation. It is not clear exactly where in the compact this Cs-134 resided, but most of the Cs measured via destructive RDLBL of this compact was in the compact core, which contained driver particles, graphitic matrix, and the DTF particles (Stempien and Cai 2024b).

The Cs-134 released from the 1400°C tests of AGR-3/4 Compacts 8-2 and 10-4 totaled 8.88E-5 (0.17 particle equivalents) and 1.25E-4 (0.24 particle equivalents), respectively. Based on the low cesium release during the AGR-1 1600°C heating tests, Cs release from the intact driver particles in AGR-3/4 Compacts 8-2 and 10-4 was not expected in any significant quantity. That the Cs-134 releases in both the 1400°C tests of AGR-3/4 Compacts 8-2 and 10-4 and the 1200°C test of AGR-3/4 Compact 10-2 exceed those from AGR-1 1600°C demonstrates how the DTF particles noticeably contributed to the overall releases from the AGR-3/4 compacts.

Comparing the four AGR-3/4 heating tests, over most of the first 48 h of each test, the Cs release rates were ordered by test temperature, meaning they were highest for the highest temperatures and lower for the lower-temperature tests. . Tests conducted at 1400°C and 1600°C saw their Cs-134 release rates peak immediately upon reaching the isothermal hold. The 1200°C test peaked within about the first 8 h of attaining the isothermal hold temperature. The peak rates ranged from 7.9E-7 to 1.3E-5 compact fraction/h, all of which are higher than the maximum Cs-134 release rates measured from all the AGR-1 1600°C and 1700°C safety tests, for which there were no SiC or TRISO failures (Morris et al. 2016). The maximum rate of 1.3E-5 h^{-1} for Compact 3-2 is higher than in any AGR-1 test from 1600°C to 1800°C, regardless of how many SiC or TRISO failures were encountered (Morris et al. 2016).

After peaking, the AGR-3/4 rates decreased steadily throughout the remainder of the tests. The AGR-1 1600°C and 1700°C tests, for which there were no SiC or TRISO failures, saw their rates level off at around 5E-9 or less. Here, the Cs-134 release rate from these AGR-3/4 compacts stayed above 1E-7 h^{-1}, except for Compact 10-2 (1200°C), which got as low as about 9E-9 h^{-1}. These AGR-3/4 rates more closely resemble the Cs-134 rates seen after SiC failure(s) during the 1600°C and 1700°C AGR-1 safety tests (Morris et al. 2016). In the AGR-3/4 results, these rates can be attributed to the DTF particles. Recall that AGR-3/4 Compact 3-2 was held at 1600°C until 335.5 hours when the temperature was raised to 1700°C. Upon reaching 1700°C, the Cs-134 release rate increased to match its initial peak of 1.3E-5 compact fraction/h at 8.5 hours. Then, while the compact was still at 1700°C, the release rate dropped to 4.3E-7 compact fraction/h, suggesting that the transportable Cs-134 (either from the DTF particles and/or the compact matrix) was being depleted when the temperature was raised to 1700°C.

AGR-1 safety test data and post-test compact analysis (including gamma counting of individual particles that experienced SiC failure) indicate that the level of cesium released from particles that experienced SiC failure at 1600–1800°C can vary from approximately 10% to 90% (Hunn et al. 2016). The pyrocarbon layer applied to the AGR-3/4 DTF particles would not substantially retain Cs, even if it remained intact, and available evidence leads to the conclusion that all DTF particles in all compacts had failed. The fact that less than 1 particle worth of Cs release was measured in these heating tests means that nearly all the Cs inventory in the DTF particles was released during the irradiation, leaving little available for release during the post-irradiation heating tests. Table 8 shows that, on average, more than half the Cs inventory produced in the DTF particles was released from the Capsule 8 and 10 compacts during irradiation (Stempien et al. 2018b).[a] The total Cs inventory that was in these FACS-tested compacts but outside the driver particle SiC layers was determined via RDLBL, and this was a small amount: approximately 0.8 to 2.8 particle equivalents (Hunn et al. 2020; Helmreich et al. 2022; Stempien and Cai 2024b). If combining the FACS release with the RDLBL inventory can serve as an estimate of the total amount of Cs-134 retained in the compacts after irradiation, that comes out to between 0.86 and 3.32 particle equivalents (4–17% of the DTF inventory) for these four compacts. This accounting confirms that only a little Cs-134 from the DTF particles was retained in the fuel compacts after irradiation, but as the RDLBL results show, most of that actually remained in the compact even after FACS testing.

[a] This determination was made by dividing the mass balance for each capsule by the number of compacts per capsule (four).

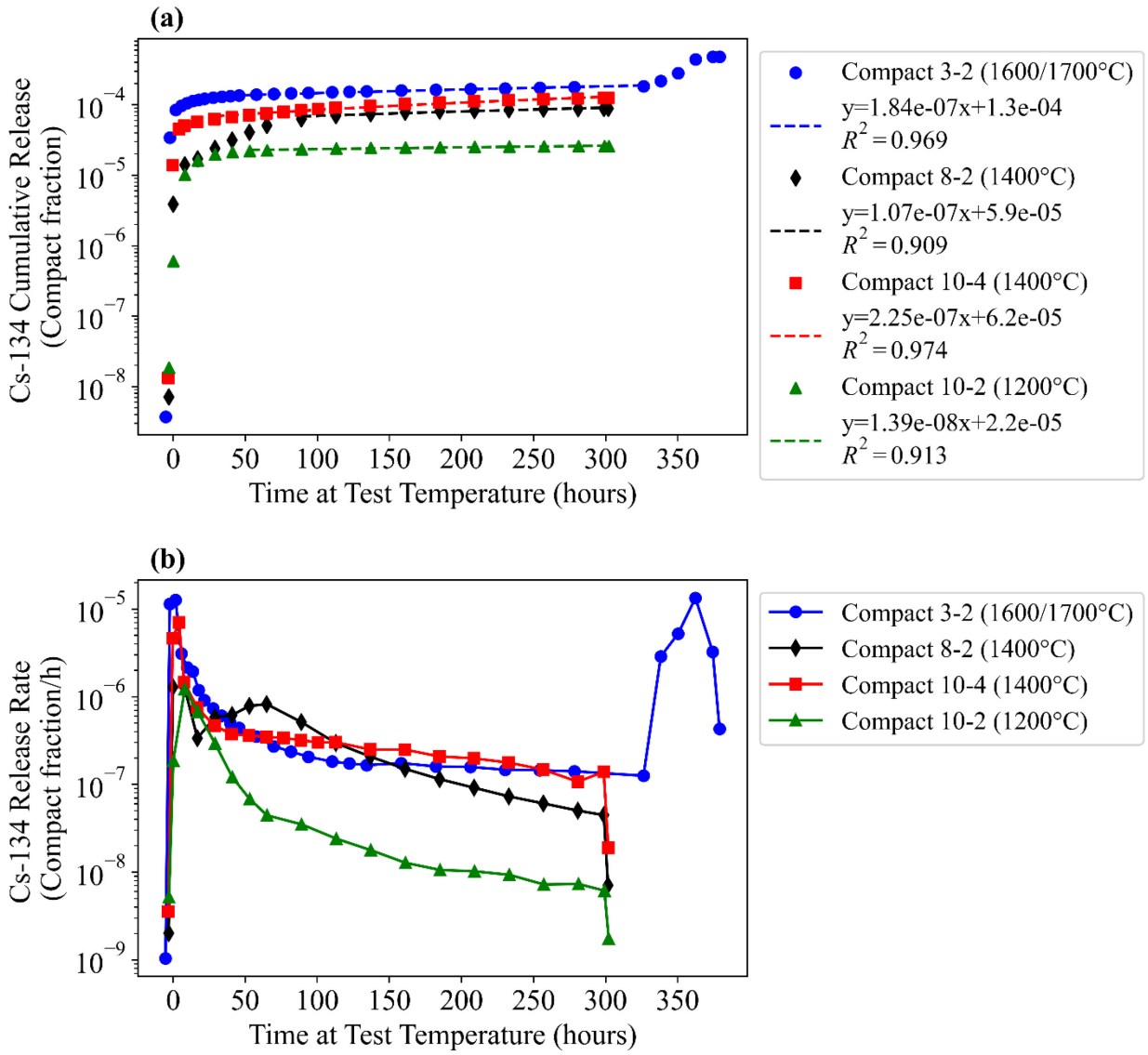

Figure 14. Cs-134 (a) release fractions and (b) release rates for the AGR-3/4 compacts.

Table 8. Summary of Cs release during the FACS tests; Cs retention in the matrix outside of driver particle SiC layers determined via RDLBL (Hunn et al. 2020; Helmreich et al. 2022; Stempien and Cai 2024b); and Cs released from an average Capsule 3, 8, or 10 compact during irradiation, based on the capsule mass balance (Stempien et al. 2018b).

Compact	Particle Equivalents		
	FACS Release	Post-FACS RDLBL	Average Release from a Compact In-pile
3-2	0.92	2.40	9.09
8-2	0.17	2.85	13.26
10-4	0.24	0.96	11.00
10-2	4.96E-2	0.81	

Figure 15 and Figure 16 plot the total Cs-134 release and the average pseudo-steady state release rates from furnace tests against EOI irradiation conditions. The beginning of Section 4 described how these

rates were determined. Note that AGR-2 Compact 6-4-2 (labeled in the plots) had no SiC or TRISO failures during its 1600°C safety test, but it was affected by cross-contamination from a preceding test that artificially elevated its Cs-134 release to about 6E-5 (Hunn et al. 2017; Stempien et al. 2021a). Similarly, AGR-2 Compact 6-4-3 (the only AGR-2 compact tested at 1800°C without any SiC failure) had a slightly elevated total Cs-134 release of about 2E-5. This slightly elevated amount of Cs was attributed to contamination picked up in the furnace at the end of the test (Hunn et al. 2019).

In these plots, it is difficult to identify trends in the post-irradiation heating test results that are linked to the fuel EOI irradiation properties (burnup and TAVA temperature), but they provide a visual summary to aid in the comparison of AGR-1, AGR-2, and AGR-3/4.

Fission-product Cs is well-retained by intact SiC layers. The total Cs release from AGR-1 and AGR-2 fell into two regions: compacts with SiC failure(s) had a total release >1E-4 compact fraction, whereas compacts with no SiC failure generally had a total fractional release of ≤1E-5. The only exceptions to that are AGR-2 Compacts 6-4-2 and 6-4-3 which had no SiC failure but had slightly elevated Cs release (>1E-5) attributed to contamination in the furnace. AGR-3/4 Compacts 3-2, 8-2, and 10-4 (FACS tested at 1600°C or 1400°C) had total Cs-134 releases similar to those in AGR-1 and AGR-2 compacts with SiC failure(s). AGR-3/4 Compact 10-2 (1200°C) had a total Cs-134 release fraction greater than most of the AGR-1 and AGR-2 compacts with no SiC failure that were tested at 1600°C, but it was less than the AGR-1 and AGR-2 compacts with SiC failure(s) at test temperatures from 1600−1800°C. The exception is that AGR-2 Compact 6-4-2 had no SiC or TRISO failures, but it had a higher Cs-134 release fraction than Compact 10-2. The average Cs-134 release rates from the AGR-3/4 compacts are generally in the same range as those from the AGR-1 and AGR-2 tests at 1600°C–1800°C, with SiC failure(s). This comparison shows that a compact with 1% of its kernels exposed in-pile has similar Cs release at 1400°C and 1600°C as a compact with about 0.02–0.1% SiC failure at 1600–1800°C.

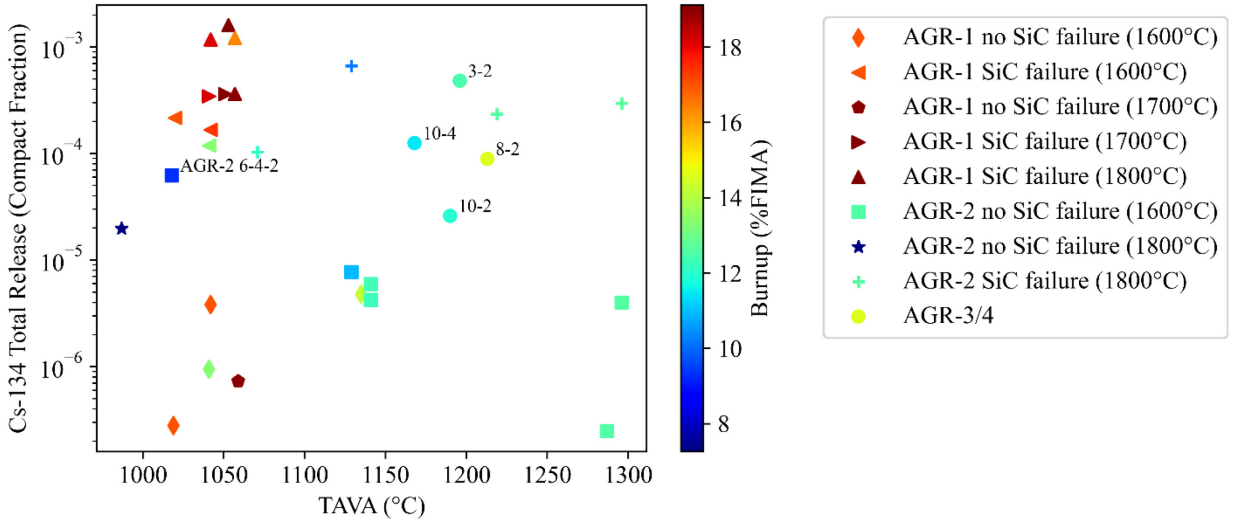

Figure 15. Total Cs-134 release during post-irradiation AGR-3/4 heating tests and post-irradiation AGR-1 and AGR-2 safety tests as a function of compact TAVA temperature and burnup. The compact ID is labeled next to the four AGR-3/4 compacts in the plot. The legend also indicates whether the tested compacts experienced SiC failure.

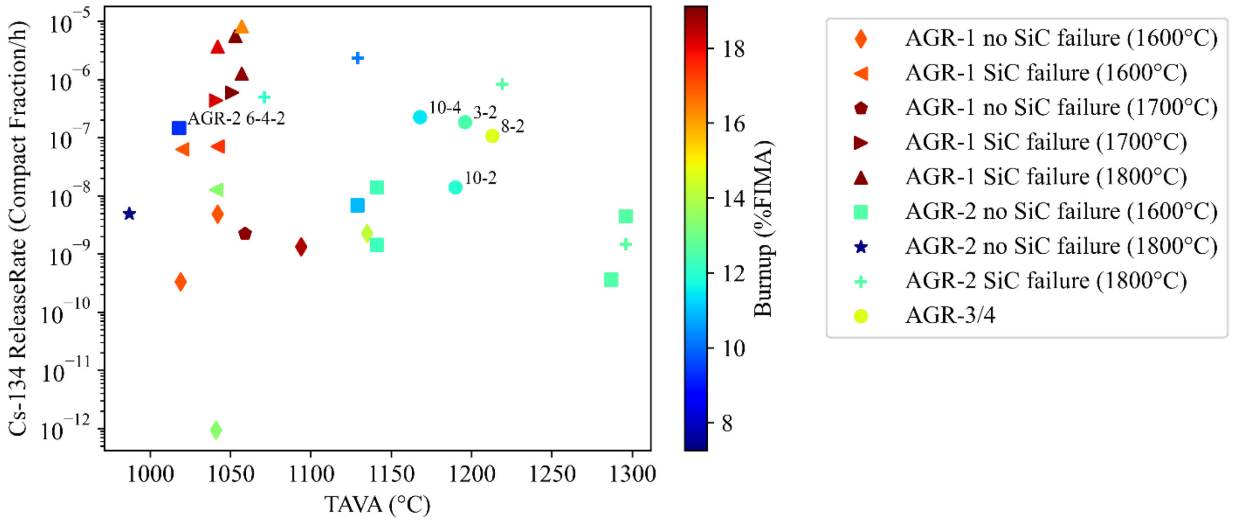

Figure 16. Average pseudo-steady-state Cs-134 release rates from post-irradiation AGR-3/4 heating tests and post-irradiation AGR-1 and AGR-2 safety tests as a function of compact TAVA temperature and burnup. The compact ID is labeled next to the four AGR-3/4 compacts in the plot. The legend also indicates whether the tested compacts experienced SiC failure.

4.3. Europium and Strontium

Figure 17 shows the release rates and total released fractions of Eu-154 and Sr-90. The fractional releases and release rates of Eu-154 and Sr-90 were similar from the same compact, and they increased with increasing test temperature. The fractions of Eu released from AGR-3/4 Compact 10-4 (1400°C) and Compact 10-2 (1200°C) are much lower than from the hotter 1600°C AGR-1 tests, where releases ranged from approximately 3E-4 to 3E-3 (Morris et al. 2016). The amount of Eu-154 released from the 1600/1700°C test of AGR-3/4 Compact 3-2 was 5.55E-3 during just the 1600°C period, and 2.22E-3 during the 1700°C period, for a total of 7.76E-3. This amount is considerably higher than in the AGR-1 1600°C tests, but less than the approximately 2E-2 fraction released from the AGR-1 1800°C tests, in which diffusive Eu release from intact TRISO particles was significant, especially from Variant 3 AGR-1 fuel (Demkowicz et al. 2015a; Stempien, Cai, and Demkowicz 2023). The AGR-1 Sr-90 release fractions ranged from 1E-5 to 3E-3 in the AGR-1 1600°C tests (Morris et al. 2016). The 1400°C test on AGR-3/4 Compact 10-4 had a Sr-90 release near the low end of that range (at 4.2E-5), and the 1600°C test of AGR-3/4 Compact 3-2 had a Sr-90 release fraction exceeding the high end of that range (at 8.2E-3). The 1600°C AGR-3/4 test had Sr-90 releases almost 3x higher than the highest Sr-90 release from the 1600°C AGR-1 testing.

Depending on the irradiation history of a given compact, the amount of Sr-90 and Eu-154 released from driver particles and retained in the compact matrix may vary from less than 0.1% to approximately 10% (Demkowicz et al. 2016; Hunn et al. 2018; Stempien, Cai, and Demkowicz 2023). Thus, it can be difficult to distinguish Eu-154 and Sr-90 releases from the 1% of DTF particles in AGR-3/4 compacts from those due to driver particles. This was certainly true for the AGR-3/4 Compact 10-2 1200°C and Compact 10-4 1400°C tests, where relatively little Eu and Sr release was measured from their FACS tests, and there were no AGR-1 or AGR-2 data for comparison in that temperature range. The observed release will be a combination of inventory that originated in the DTF particles that was retained following irradiation plus inventory produced in the TRISO-coated driver particles that diffused through intact coatings and was retained in the compact. Which of those sources is dominant may not be obvious.

Figure 18 and Figure 19 compare total Eu and Sr releases among AGR-1, AGR-2, and the four as-irradiated AGR-3/4 compacts that were subjected to post-irradiation heating. Figure 20 and Figure 21 summarize some average releases from the pseudo-steady-state periods of these tests. Table 9 summarizes the releases measured from the AGR-3/4 FACS tests; the retention in the matrix outside of the driver-particle SiC layers, as determined via AGR-3/4 RDLBL (Hunn et al. 2020; Helmreich et al. 2022; Stempien and Cai 2024b); and the amount released from an average compact in AGR-3/4 Capsules 3, 8, and 10 during irradiation, based on the mass balance (Stempien et al. 2018b). Unlike Ag-110m, for instance, the Eu-154 release rates during post-irradiation heating tests somewhat depend on the prior irradiation temperature (Stempien, Cai, and Demkowicz 2023). This adds a layer of complexity when comparing the Eu and Sr releases from these four AGR-3/4 compacts (irradiated at temperatures averaging about 1200°C) with those from AGR-1 compacts (mostly irradiated at about 1050°C). In addition to the DTF particles, which have lesser—though not negligible—Eu and Sr retention than TRISO-coated particles, the AGR-3/4 compacts tested here had higher irradiation temperatures. Stempien et al. (2023) compiled data from AGR-1, AGR-2, and AGR-3/4 and noted that there appeared to be a threshold above which safety tests (especially 1600°C safety tests) of compacts irradiated at TAVA temperatures of >1200°C show distinctly higher release rates than those from compacts irradiated at TAVA temperatures <1200°C. The reason hotter fuel has higher safety test release rates is because the in-pile rate of Eu-154 accumulation in the OPyC and fuel compact matrix increases with irradiation temperature and accelerates dramatically above 1200°C (Stempien, Cai, and Demkowicz 2023). This is from an increase in both Eu and Sr release through intact particles and an increase in the release of those nuclides from the compact.

AGR-3/4 Compact 3-2 released noticeably more Eu and Sr during its 1600/1700°C test than the tests of AGR-1 compacts at 1600°C and 1700°C. In addition to the DTF particles, AGR-3/4 Compact 3-2 had a significantly higher irradiation temperature than the AGR-1 compacts. Table 9 shows that a total of about 34 particle equivalents of Eu and 31 of Sr-90 (a fraction of about 1.8E-2) were detected as having been released in-pile, released during FACS testing, or measured during destructive RDLBL (Stempien and Cai 2024b). With only 20 DTF particles per compact, this is evidence of Sr-90 and Eu-154 diffusion through intact TRISO coatings. Except for AGR-1 Compact 6-1-1, which had a fraction of 1.5E-2 Eu-154 (but only 5.9E-4 Sr-90), the rest of the AGR-1 as-irradiated (i.e., not safety tested) DLBL exams showed Eu-154 present in the compacts at between 2.4E-4 and 1.2E-3 (Demkowicz et al. 2015a).

The total Eu-154 and Sr-90 releases from the 1400°C tests of AGR-3/4 Compacts 8-4 and 10-2 were much lower than for AGR-3/4 Compact 3-2, yet they were still comparable to the low end of the range of total releases from some 1600°C tests of AGR-1 and AGR-2 fuel. During the 1600°C portion of the Compact 3-2 test, the Eu-154 release rates were several times higher than for the AGR-1 1600°C tests, where rates ranged from 1E-6 to 1E-5 compact fraction/h (Morris et al. 2016). The AGR-3/4 Compact 3-2 rates at 1600°C were comparable to the early release rates (time < 125 h) from the AGR-1 1800°C testing (Morris et al. 2016). There was a notable increase in the AGR-3/4 Compact 3-2 Eu-154 release rate when the temperature was raised to 1700°C toward the end of the Compact 3-2 test. This rate was about 4.5E-5 compact fraction/hr (similar to the initial rate spike at the start of the test). In contrast to the cesium behavior (which decreased while the temperature was still at 1700°C), the Eu release rate remained constant for the entire period of time at 1700°C. This suggests that the source of transportable Cs within Compact 3-2 was being depleted, but that the source of Eu was not close to being depleted.

In Table 9, except for Eu-154 from Compact 10-4, the sum of Eu and Sr released during these AGR-3/4 FACS tests, retained in the compact but outside of intact TRISO SiC coatings, and released in-pile exceeded 20 particle equivalents. This is evidence of release of these nuclides through intact TRISO SiC coatings. However, the amount of Eu and Sr measured via RDLBL shows how well it is still retained in the compacts. Compact 8-2 had about 53 particle equivalents of Eu-154 and Sr-90 in the compact matrix and OPyC, but it released less than 1 particle equivalent during its 1400°C FACS test. By comparison, AGR-3/4 Compact 3-2 had less inventory remaining in the compact matrix and OPyC, and it

released about 15 particle equivalents of Eu and Sr in its FACS test. This is evidence of a significant further acceleration in the Eu and Sr release rates at between 1400°C and 1600°C.

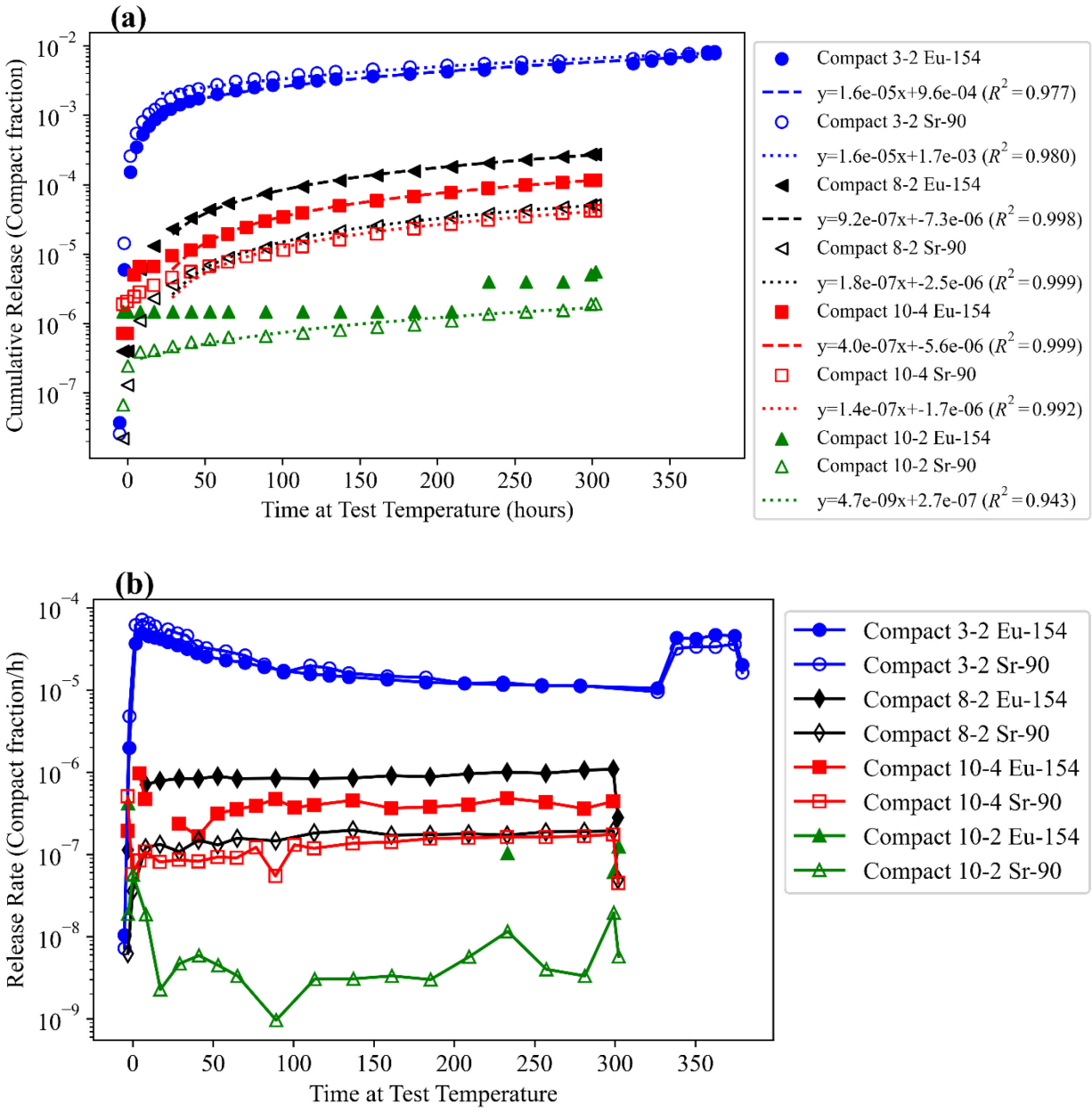

Figure 17. Eu-154 and Sr-90 (a) release fractions and (b) release rates from the AGR-3/4 FACS tests. Note that only four condensation plates from the Compact 10-2 test had measurable Eu-154.

Table 9. Summary of Eu and Sr release during the FACS tests; retention in the matrix outside of driver particle SiC layers, as determined via RDLBL (Hunn et al. 2020; Helmreich et al. 2022; Stempien and Cai 2024b); and average in-pile release, based on the capsule mass balances (Stempien et al. 2018b).

Compact	Eu-154 Particle Equivalents			Sr-90 Particle Equivalents		
	FACS Release	Post-FACS RDLBL	Avg In-pile Release	FACS Release	Post-FACS RDLBL	Avg In-pile Release
3-2	14.89	10.53	8.95	15.76	6.54	8.43
8-2	0.52	53.19	2.8	0.10	52.43	3.7
10-4	0.22	13.98	2.32	0.08	14.34	7.04
10-2	1.06E-2	26.54		3.67E-3	22.43	

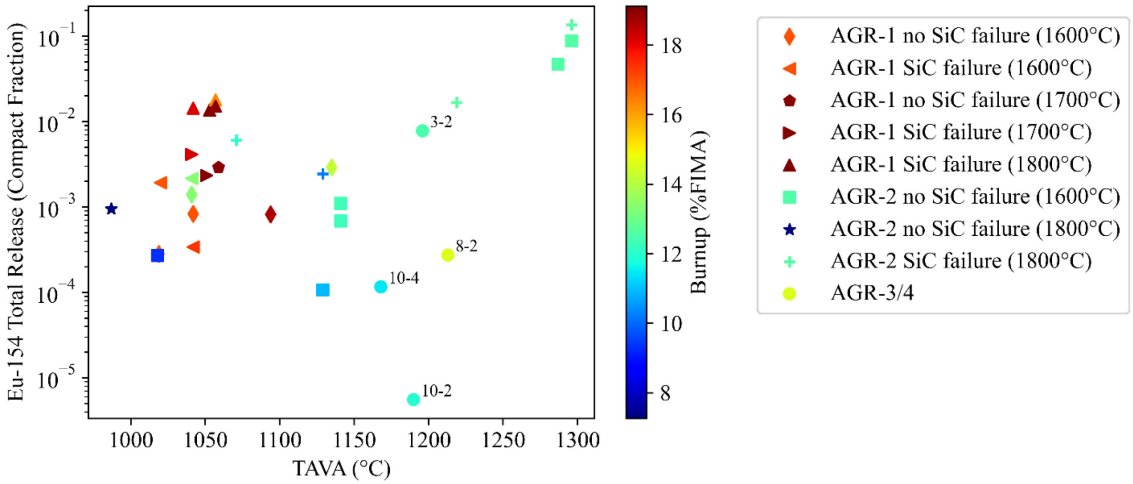

Figure 18. Total Eu-154 release during the post-irradiation AGR-3/4 heating tests and post-irradiation AGR-1 and AGR-2 safety tests as a function of compact TAVA temperature and burnup. The compact ID is labeled next to the four AGR-3/4 compacts in the plot. The legend also indicates whether the tested compacts experienced SiC failure.

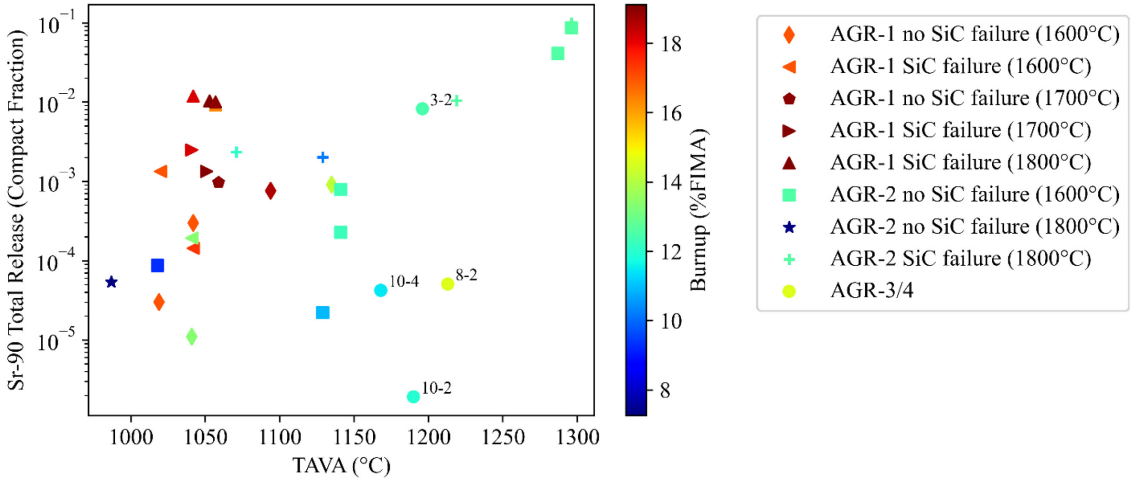

Figure 19. Total Sr-90 release during post-irradiation AGR-3/4 heating tests and post-irradiation AGR-1 and AGR-2 safety tests as a function of compact TAVA temperature and burnup. The compact ID is labelled next to the four AGR-3/4 compacts in the plot. The legend also indicates whether the tested compacts experienced SiC failure.

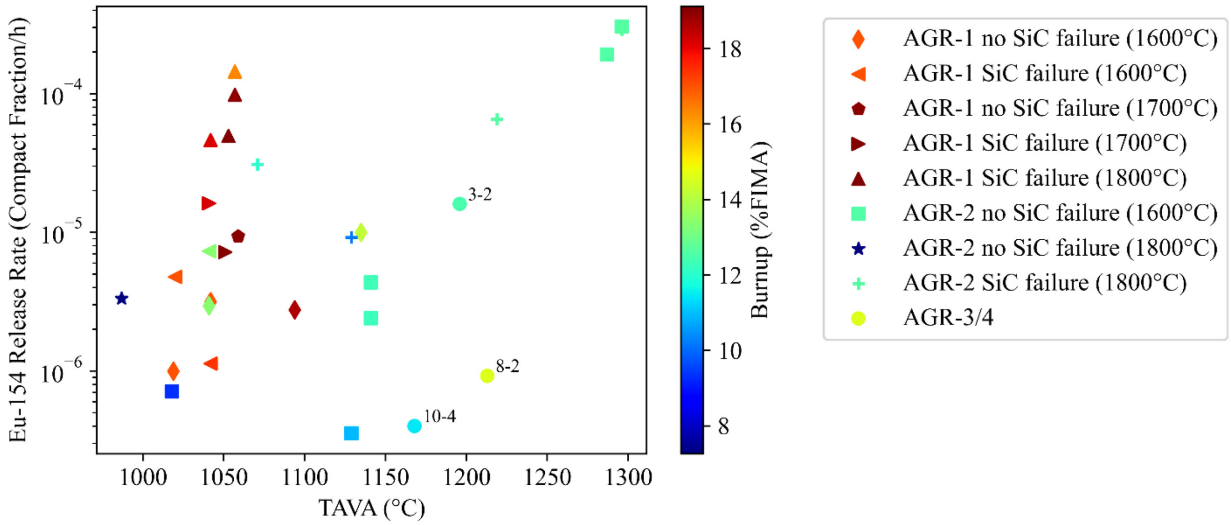

Figure 20. Average pseudo-steady-state Eu-154 release rates during post-irradiation AGR-3/4 heating tests and post-irradiation AGR-1 and AGR-2 safety tests as a function of compact TAVA temperature and burnup. The compact ID is labeled next to the four AGR-3/4 compacts in the plot. The legend also indicates whether the tested compacts experienced SiC failure. Eu-154 was only detected on four of the condensation plates from the AGR-3/4 Compact 10-2 test. Thus, an average was not computed for it.

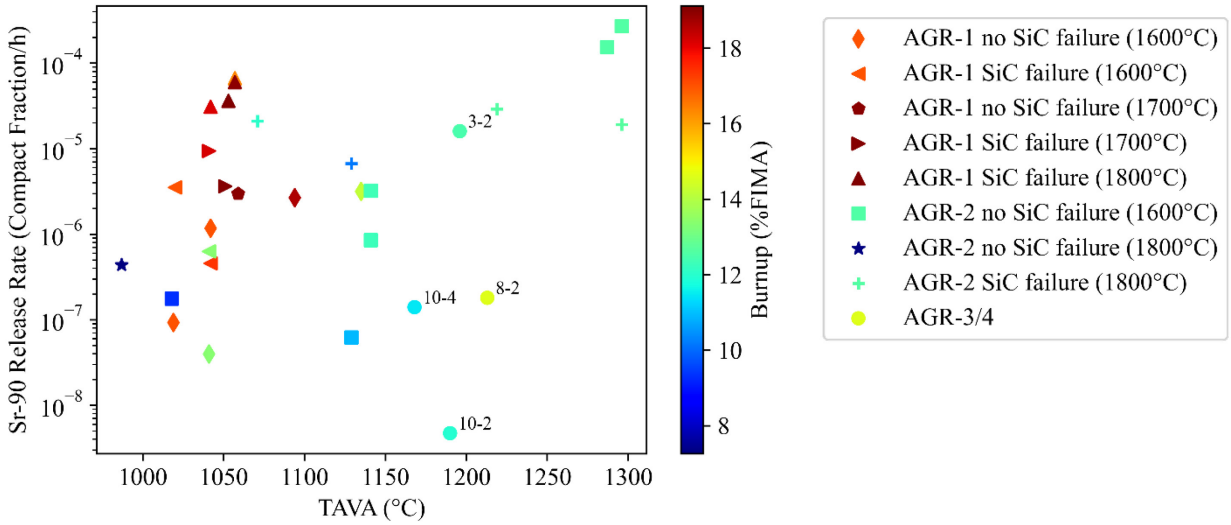

Figure 21. Average pseudo-steady-state Sr-90 release rates during the post-irradiation AGR-3/4 heating tests and post-irradiation AGR-1 and AGR-2 safety tests as a function of compact TAVA temperature and burnup. The compact ID is labelled next to the four AGR-3/4 compacts in the plot. The legend also indicates whether the tested compacts experienced SiC failure.

4.4. Antimony

Fission-product antimony (Sb-125) has not received as much attention as other nuclides in previous AGR post-irradiation heating tests, largely because it is seldom observed in the gamma spectra of condensation plates. However, given the seemingly consistent measurements from the set of four AGR-3/4 FACS tests, it is worth including here. This nuclide decays via β^- emission, but it has some

gamma rays associated with that decay. The total Sb-125 releases were highest for Compacts 3-2 (1600/1700°C FACS) and 10-4 (1400°C FACS). The initial rate for Compact 3-2 was highest of all, but Compact 10-4 had a little higher rate shortly after reaching the isothermal hold and for the remainder of that hold. The 1200°C test of Compact 10-2 showed a level of Sb-125 release about two orders of magnitude less than the 1400°C and 1600/1700°C tests.

At 1600°C, the amount of Sb-125 released from Compact 3-2 exceeded that of any other fission-product radionuclides observed in these tests except Eu-154, Eu-155, and Sr-90. In both 1400°C tests, the amount of Sb-124 release was more than other nuclides except Ag-110m. At 1200°C, only small quantities of nuclides other than Ag-110m were released, and Sb-125 was the highest among them (at 0.07 particle equivalents). Because of the DTF particles, more Sb-125 release was seen in AGR-3/4 than in AGR-1 (as with Cs-134); however, judging by the total amount of Sb-125 released from the FACS tests, the amount of Sb-125 retained in the compacts after irradiation was greater than for Cs-134, making the total release potential for Sb-125 greater in post-irradiation heating than for Cs-134.

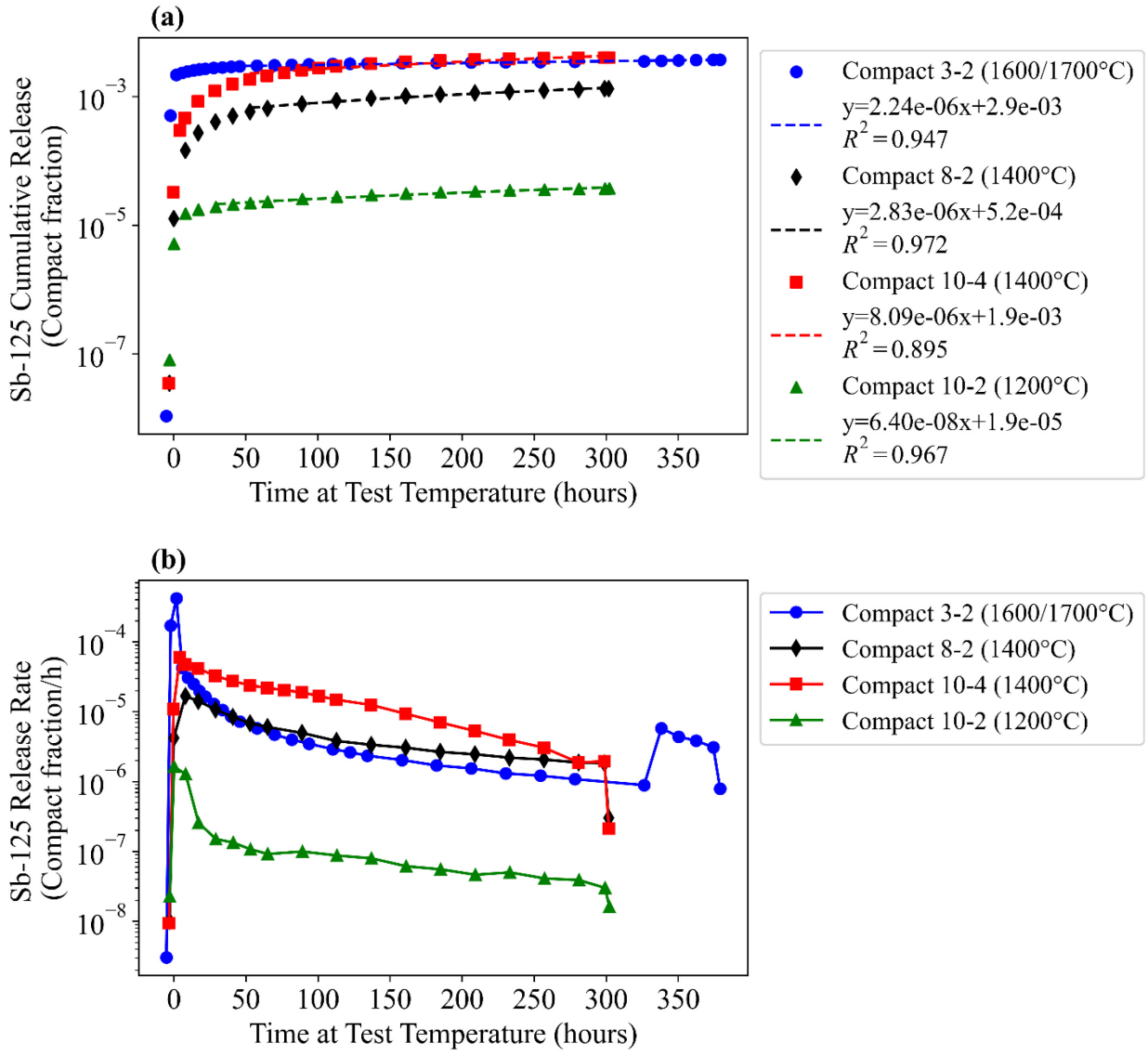

Figure 22. Sb-125 (a) release fractions and (b) release rates from AGR-3/4 FACS tests.

4.5. Krypton

Figure 23 shows the Kr-85 release fraction vs. time for the AGR-3/4 fuel compacts heated in the FACS furnace. Because all the Kr-85 was collected in a single cold trap, there were point-to-point variations (within the statistical accuracy of the system) in the total Kr-85 detected in the traps as a function of time. Thus, the cumulative Kr-85 release was plotted, and linear fits were used to determine release rates for specific periods of each test where the slope of the release-vs.-time plot significantly changed. These rates are summarized in Table 10.

The total Kr-85 release increased with increasing test temperature and tended to track along with the Cs-134 release. This is apparent in the summary plots given for each test in Sections 3.1–3.4. Total Kr-85 fractions of 1.43E-4 (0.27 particle equivalents) and 1.53E-4 (0.290 particle equivalents) were released from AGR-3/4 Compacts 8-2 (1400°C) and 10-4 (1400°C), respectively—slightly less than the 1.64E-4 (0.32 particle equivalents) released from the 1600°C period of the test of AGR-3/4 Compact 3-2. A lower fraction of 2.65E-5 (0.051 particle equivalents) was released from the 1200°C test of Compact 10-2. For comparison, during 1600°C testing of AGR-1 compacts, the fractional Kr-85 releases were considerably lower: approximately 1E-6 to 5E-6 after 300 hours (Morris et al. 2016). Given that the fraction of Kr-85 released from AGR-3/4 compacts at 1400°C and 1600°C was significantly higher than from AGR-1 1600°C tests, this indicates that most of the measured Kr-85 from AGR-3/4 compacts was due to release of the remaining Kr-85 inventory in the DTF particle fuel kernels. Given that the AGR-3/4 test with the highest Kr-85 release was only 37% of a single particle, it is concluded that the majority of the Kr-85 had been released from the DTF particles during irradiation.

Early in the tests (during Period I, shown in Figure 23[b]), the Compact 10-2 (1200°C) Kr-85 release rate was 2.4E-6 h^{-1}, which is about 2x lower than for Compact 10-4 (1400°C) and 5x lower than for Compact 3-2 (1600/1700°C). Interestingly, the Period-I release rate from Compact 10-2 was 1.5x higher than for Compact 8-2 (1400°C); however, for Periods II+, the Compact 8-2 rate was much higher. For all the compacts, the release rate slowed down for Period II in comparison to Period I. For the remainder of the Compact 10-2 test (Period II), the rates were 10–20x lower than the Period II and III rates from the other three tests. For compacts tested at or above 1400°C, there was an additional period (Period III) in which the release rate slowed further compared to Period II. For Compact 3-2, Periods IV and V were responses to increasing the test temperature from 1600°C to 1700°C. After the initial increase of more than an order of magnitude from Period III (1600°C) to Period IV (ramp from 1600°C to 1700°C), the release rate in Period V slowed down to match that in Period II (i.e., 3E-7 h^{-1}). The AGR-3/4 Kr-85 release rates generally exceeded those observed at 1600°C from the AGR-1 safety tests. In the AGR-1 1600°C tests, the Kr-85 release rates were on the order of 1E-9 h^{-1}, there were few SiC failures (the observed SiC failure fraction was 9.4E-5), and there were no TRISO failures (Demkowicz et al. 2015a; Stempien, Cai, and Demkowicz 2023). The release rates for AGR-3/4 Compacts 3-2, 8-2, and 10-4 exceeded those for the 1700°C AGR-1 safety tests, which had Kr-85 release rates on the order of 1E-8 h^{-1}, no TRISO failures, and the observed SiC failure fraction was 5.6E-4 (Hunn et al. 2013; Hunn et al. 2015b; Demkowicz et al. 2015a). This further supports the inference that the 20 exposed kernels in the DTF particles did retain small but measurable amounts of Kr-85.

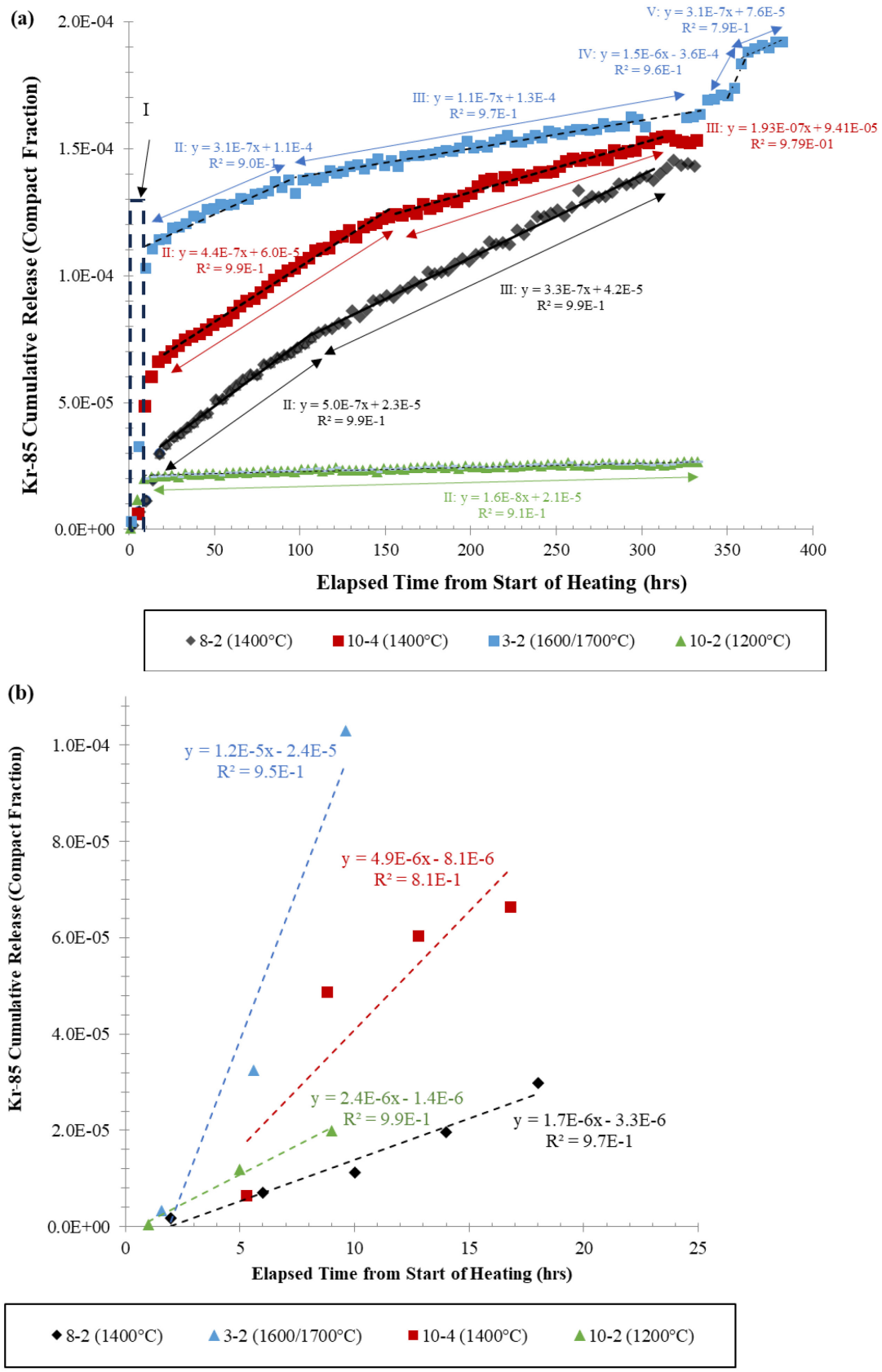

Figure 23. (a) Kr-85 release from each test. Regions are labeled I through V. (b) Region I only.

Table 10. Kr-85 release rates (fraction/h) from specific portions of each test. Regions I through V correspond to Figure 23a.

	Burnup (% FIMA)	TAVA (°C)	FACS Temp (°C)	I	II	III	IV	V
3-2	12.49	1196	1600/1700	1.2E-5	3.1E-7	1.1E-7	1.5E-6	3.1E-7
8-2	14.58	1213	1400	1.7E-6	5.0E-7	3.3E-7	N/A	N/A
10-4	11.43	1168	1400	4.9E-6	4.4E-7	1.9E-7	N/A	N/A
10-2	11.96	1190	1200	2.4E-6	1.6E-8	N/A	N/A	N/A

N/A: not applicable

5. SUMMARY AND CONCLUSIONS

Four irradiated AGR-3/4 compacts, each with 20 DTF particles were heated to temperatures between 1200°C and 1700°C. All isothermal periods were held for 300 h (except for the additional 48-h hold at 1700°C for Compact 3-2), and the condensable and gaseous fission-product releases were measured.

In each test, the Ag-110m release rates were highest during the ramp to test temperature. After reaching the test temperature, the release rates were noticeably lower and tended to decrease with increasing time at the isothermal holds, presumably as the major sources of the Ag-110m were being depleted. The total releases and release rates of Ag-110m were highest for the 1200°C test of AGR-3/4 Compact 10-2. These Ag-110m release rates compared well with previous AGR-1 safety tests and further supported the observation that Ag-110m rates are highest in the intermediate temperature range of 1100–1300°C.

Consistent with the AGR-1 and AGR-2 safety tests, the total releases of Cs, Eu, Sr, and Kr from the AGR-3/4 compacts generally increased with post-irradiation test temperature. The total Kr-85 release increased with increasing test temperature and tended to track along with the total amount of Cs-134 released from the same test. The total releases of Kr-85 from the AGR-3/4 compacts are higher than from the AGR-1 and AGR-2 compact safety tests, for which there were no TRISO failures. These higher Kr-85 releases from AGR-3/4 can be attributed to the DTF fuel particles in the AGR-3/4 compacts, which retained small but noticeable quantities of Kr-85 (~0.3 particle equivalents).

In these AGR-3/4 heating tests, the Cs-134 release rates increased with increasing test temperature. Tests conducted at 1400°C and 1600°C saw their highest Cs-134 release rates immediately upon reaching the isothermal hold. The 1200°C test peaked within about the first 8 h of attaining the isothermal hold temperature. Cs-134 releases from the heating tests ranged from 0.05 to 0.9 particle equivalents. Post-test RDLBL of these compacts measured 0.8–2.8 particle equivalents of Cs-134, meaning that 4–14% of the inventory of exposed kernels was retained in the compacts after irradiation and subsequent post-irradiation heating. Combining the RDLBL and FACS-test measurements reveals that that 0.86 and 3.32 particle equivalents (4–17% of the DTF inventory) were retained in the fuel compacts after irradiation.

Prior work found that the amount of Sr-90 and Eu-154 released from driver particles and retained in the compact matrix after irradiation may vary from <0.1% up to approximately 10%, depending on the irradiation history of a given compact (Demkowicz et al. 2016; Hunn et al. 2018; Stempien, Cai, and Demkowicz 2023). Compacts with irradiation temperatures >1200°C had considerably more Sr and Eu in the matrix outside of intact SiC layers than compacts with lower irradiation temperatures. The AGR-3/4 compacts tested here had average irradiation temperatures of about 1200°C, whereas those from AGR-1 had ones of about 1050°C. Thus, it can be difficult to distinguish Eu-154 and Sr-90 releases originating from the 1% of DTF particles in AGR-3/4 compacts from those originating from the driver particles, especially if the FACS-releases were ≤1%. On the other hand, if considerably more than 1% of the

compact fraction of Eu or Sr was measured, that excess can be attributed to the TRISO-coated driver particles.

AGR-3/4 compacts tested at temperatures of 1200°C and 1400°C were found to have relatively low Eu and Sr releases over the ~300 h of the tests. For example, Compact 8-2 had about 53 particle equivalents of Eu-154 and Sr-90 in the compact matrix, OPyC, and DTF particles after irradiation and FACS testing, but it released less than 1 particle equivalent during its 1400°C FACS test. The Eu and Sr release rates appeared to accelerate between 1400°C and 1600°C. The amount of Eu-154 released from the 1600/1700°C test of AGR-3/4 Compact 3-2 was 5.55E-3 during just the 1600°C period, and 2.22E-3 during the 1700°C period, for a total of 7.76E-3. This amount is considerably more than in the AGR-1 1600°C tests, but less than the ~2E-2 fraction released from AGR-1 1800°C tests, where diffusive Eu release from intact TRISO particles was significant, especially from Variant 3 AGR-1 fuel.

Based on the results of the heating tests presented here, along with data from RDLBL analysis of as-irradiated and furnace-tested fuel compacts and the capsule mass balance report, the following observations and conclusions regarding fission product behavior can be made.

Silver:

- Most of the Ag-110m generated in these compacts was released during irradiation in ATR. Because of the substantial in-pile release rate from intact driver particles during irradiation, it is not possible to determine the relative contributions to the heating test release from DTF particles (which constituted about 1% of the particles in the compacts), driver particles, or silver inventory retained in the OPyC or matrix. Nonetheless, the release behavior during these heating tests is consistent with previous observations that a maximum rate of release from intact TRISO particles occurs at intermediate temperatures of 1100–1300 °C.
- These results demonstrate that assessing Ag behavior in exposed kernels is difficult even with ~1% DTF present because of the significant release fraction from intact TRISO particles, which can reach tens of percent.

Cesium:

- While there was little DTF-particle Cs-134 inventory remaining in the compacts at the end of irradiation, the majority of that inventory remained in the compacts during the heating tests and was found in the core section of compacts during post-test destructive analysis. As a result, these heating tests represent release from the small remainder of inventory in the compacts at the end of irradiation (residing either in the DTF particles or the compact matrix) and may not be representative of the release immediately following a TRISO particle failure.

Europium and strontium:

- The in-pile release of appreciable quantities of Eu and Sr from intact driver particles and the relatively high level of retention of these elements in the OPyC and/or matrix makes it difficult to ascertain the source of release during the heating tests because DTF particles, driver particles, and stored inventory in the OPyC/matrix can all contribute to observed releases.
- For post-irradiation exposures ≤1400°C for up to 300 hours, very little of the exposed Eu and Sr inventories (meaning inventories in the compact outside of the SiC coatings of intact driver particles) is released from the fuel compacts, indicating good retention in the DTF kernels and/or the OPyC/matrix. Between 1400 °C and 1600 °C the release increases appreciably such that the original exposed inventory is released from the compact and additional release from intact TRISO particles may begin to contribute to both the matrix inventory and the release of that inventory from the compact altogether.

Krypton:

- Nearly all of the Kr-85 was released from the DTF particles in-pile, as there was typically less than 2% of the DTF particle inventory (compact fraction <1.9E-4) released during these heating tests. Thus, these heating tests assess the release of only the small portion of krypton that remains in the kernels and may not be representative of release rates expected from failed particles. The total release of Kr-85 from the heating tests did increase with test temperature.

Antimony:

- The release of Sb-125 appears to have its own unique behavior. The shapes of the cumulative releases vs. time tend to resemble those for Cs-134. However, the total amount of Sb-125 released from the tests at ≥1400°C is about an order of magnitude higher than the Cs-134 quantities, which suggests that exposed Sb-125 is better retained in the compact than exposed Cs-134. The destructive exams of as-irradiated compacts supports this observation. At 1200°C, the cumulative Sb-125 release was about 2 orders of magnitude lower than it is at 1400°C+, and while the cumulative Sb-125 release at 1200°C is orders of magnitude lower than Ag-110m is at 1200°C, the shape of the cumulative release vs. time curve resembles that of Ag-110m.

Ongoing work aims to compare AGR-3/4 measurements (such as those presented here) with predictions from fission product transport models and continue looking for potential effects of the irradiation history (e.g., temperature and burnup) on observed behaviors of key nuclides during post-irradiation heating tests. Attempts to derive and refine useable transport parameters from the AGR-3/4 fission product profiles are in progress. A set of five AGR-3/4 fuel compacts were reirradiated in NRAD and subsequently FACS tested. Some preliminary results have been discussed already (Stempien et al. 2021b), but a final report on those results will expand the data and analysis surrounding fission product release from exposed kernels.

6. REFERENCES

Collin, B.P., 2015a, "AGR-3/4 Irradiation Test Final As-Run Report", Idaho National Laboratory, INL/EXT-15-35550, Rev. 0, June 2015.

Collin, B.P., 2015b, "AGR-3/4 Irradiation Experiment Test Plan", Idaho National Laboratory, PLN-3867, Rev. 1, May 2015.

Collin, Blaise P., et al. 2018. "The AGR-3/4 fission product transport irradiation experiment." Nuclear Engineering and Design 327: 212-227. https://doi.org/10.1016/j.nucengdes.2017.12.016

Demkowicz, Paul A., David V. Laug, Dawn M. Scates, Edward L. Reber, Lyle G. Roybal, John B. Walter, Jason M. Harp, and Robert N. Morris. 2012. "The Fuel Accident Condition Simulator (FACS) furnace system for high temperature performance testing of VHTR fuel." Nuclear Engineering and Design, Vol. 251, pp. 164-172, 2012.

Demkowicz, P. A., et al. 2015a. "AGR-1 Post Irradiation Examination Final Report." INL/EXT-15-36407, Idaho National Laboratory, Idaho Falls, ID. https://doi.org/10.2172/1236801.

Demkowicz, Paul A., et al. 2015b. "First high temperature safety tests of AGR-1 TRISO fuel with the Fuel Accident Condition Simulator (FACS) furnace." Journal of Nuclear Materials 464: 320-330. https://doi.org/10.1016/j.jnucmat.2015.05.006.

Demkowicz, P.A. et al. 2016. "Irradiation Performance of AGR-1 High Temperature Reactor Fuel." Nuclear Engineering and Design, 306, 2-13, 2016.

Grover, Blaine, John Maki and David Petti. 2010. “Completion of the first NGNP Advanced Gas Reactor Fuel Irradiation Experiment, AGR-1, in the Advanced Test Reactor.” HTR 2010, Prague, Czech Republic, October 18-20, 2010.

Grover, S. Blaine and David A. Petti. 2014. "Status of the NGNP fuel experiment AGR-2 irradiated in the advanced test reactor." Nuclear Engineering and Design 271: 238-243. https://doi.org/10.1016/j.nucengdes.2013.11.038

Harp, Jason M., John D. Stempien, and Paul A. Demkowicz. 2021. “Gamma Spectrometry Examination of the AGR-3/4 Irradiation.” INL/EXT-20-58254, Rev. 1. Idaho National Laboratory, Idaho Falls, ID.

Hawkes, G. 2016. “AGR-3/4 Daily As-Run Thermal Analyses.” ECAR-2807, Rev. 1, Idaho National Laboratory, Idaho Falls, ID.

Helmreich, G. W., Montgomery, F. C., and J. D. Hunn. 2015. “Development of a Radial Deconsolidation Method.” ORNL/TM-2015/699, Oak Ridge National Laboratory. https://doi.org/10.2172/1235005.

Helmreich, G.W., Hunn, J.D., Montgomery, F.C., and D. J. Skitt. 2021. “Radial Deconsolidation and Leach-Burn-Leach of AGR-3/4 Compacts 8-4 and 7-4.” ORNL/TM-2021/2178, Oak Ridge National Laboratory. https://doi.org/10.2172/1820768.

Helmreich, G., Hunn, J.D., Montgomery, F. C., and D. J. Skitt. 2022. “Radial Deconsolidation and Leach-Burn-Leach of AGR-3/4 Compacts 1-3, 4-3, 10-1, and 10-2,” ORNL/TM-2022/2586, Oak Ridge National Laboratory. https://doi.org/10.2172/1887677.

Hunn, J.D., Lowden, R.A. 2007. “Data Compilation for AGR-3/4 Driver Fuel Coated Particle Composite LEU03-09T.” ORNL/TM-2007/019, Oak Ridge National Laboratory.

Hunn, J.D., Miller, J.H. 2009. “Data Compilation for AGR-3/4 Designed-to-Fail (DTF) Fuel Particle Batch LEU04-02DTF.” Oak Ridge National Laboratory, ORNL/TM-2008/193, October 2009.

Hunn, J., Trammell, M. P., Montgomery, F.C., 2011. “Data Compilation for AGR-3/4 Designed-to-Fail (DTF) Fuel Compact Lot (LEU03-10TOP2/LEU03-07DTF-OP1)-Z.” ORNL/TM-2011/124. Oak Ridge National Laboratory.

Hunn, J.D., et al. 2013. “PIE on Three Irradiated AGR-1 Compacts in FY2013.” ORNL/LTR-2013/291. Oak Ridge National Laboratory, Oak Ridge, TN

Hunn, John D., et al. 2014. "Fabrication and characterization of driver-fuel particles, designed-to-fail fuel particles, and fuel compacts for the US AGR-3/4 irradiation test." Nuclear Engineering and Design 271: 123-130. https://doi.org/10.1016/j.nucengdes.2013.11.020

Hunn, J.D., et al. 2015a. “PIE on Safety-Tested AGR-1 Compact 4-2-2.” ORNL/TM-2015/033, Oak Ridge National Laboratory.

Hunn, J.D., et al. 2015b. “PIE on Safety Tested AGR-1 Compact 5-1-1.” ORNL/TM-2015/317, Oak Ridge National Laboratory.

Hunn, J. D., C. A. Baldwin, T. J. Gerczak, F. C. Montgomery, R. N. Morris, C. M. Silva, P A. Demkowicz, J. M. Harp, and S. A. Ploger. 2016. “Detection and Analysis of Particles with Failed SiC in AGR-1 Fuel Compacts.” *Nuclear Engineering and Design* 306:36–46. https://doi.org/10.1016/j.nucengdes.2015.12.011.

Hunn, J.D., et al. 2017. “Safety-Testing of AGR-2 UCO Compacts 6-4-2 and 2-3-1.” ORNL/TM-2017/439, Revision 0. Oak Ridge National Laboratory. https://doi.org/10.2172/1376621.

Hunn, J.D., et al. 2018. “Post-Irradiation Examination and Safety Testing of US AGR-2 Irradiation Test Compacts.” HTR 2018, HTR-2018-3010, Warsaw, Poland, October 8-10, 2018.

Hunn, J.D., et al. 2019. “Safety Testing and Destructive Examination of AGR-2 UCO Compact 6-4-3.” ORNL/TM-2019/1200, Revision 0. Oak Ridge National Laboratory. https://doi.org/10.2172/1530077.

Hunn, J.D., F.C. Montgomery, D.J. Skitt, G.W. Helmreich. 2020. “Radial Deconsolidation and Leach-Burn-Leach of AGR-3/4 Compacts 1-4 and 10-4.” ORNL/TM-2020/1707, Oak Ridge National Laboratory. https://doi.org/10.2172/1709104.

Morris, R.N., et al. 2016. “Performance of AGR-1 high temperature reactor fuel during post-irradiation heating tests.” Nuclear Engineering and Design 306, 24-35, 2016.

Pham, Cam Binh T., Joe Palmer, Douglas W. Marshall, Grant L. Hawkes, Dawn M. Scates, and Paul A. Demkowicz. 2021. “AGR-5/6/7 Irradiation Test Final As-run Report.” INL/EXT-21-64221, Idaho National Laboratory, September 2021.

Stempien, J. D. 2017. “Radial Deconsolidation and Leach-burn-leach of AGR-3/4 Compacts 3-3, 12-1, and 12-3.” INL/EXT-17-43182, Idaho National Laboratory, Idaho Falls, ID. https://doi.org/10.2172/1408764.

Stempien, J.D., Demkowicz, P.A., Reber, R.L., Christensen, C.L., 2018a “Preliminary results from the first round of post-irradiation heating tests of fuel compacts from the US AGR-3/4 irradiation,” Proceedings of HTR 2018, Paper HTR 2018-323, October 2018. https://www.osti.gov/biblio/1478513

Stempien, J.D., Demkowicz, P.A., Harp, J.M., Winston, Philip L., 2018b “AGR-3/4 Experiment Preliminary Mass Balance,” INL/EXT-18-46049, August 2018.

Stempien, John D. and Jason Schulthess. 2020. “AGR-3/4 TRISO Fuel Compact Ceramography.” INL/EXT-20-57610.

Stempien, J. D., J. D. Hunn, R. N. Morris, T. J. Gerczak, and P. A. Demkowicz. 2021a. “AGR-2 TRISO Fuel Post-Irradiation Examination Final Report.” INL/EXT-21-64279, Idaho National Laboratory, Idaho Falls, ID. https://www.osti.gov/biblio/1822447.

Stempien, John D., Paul A. Demkowicz, Edward L. Reber, and Cad L. Christensen. 2021b. “Reirradiation and Heating Testing of AGR-3/4 TRISO Fuels.” Proceedings of HTR 2021, Paper HTR2021-3004. Yogyakarta, Indonesia, June 2-4, 2021.

Stempien, J. D., Cai, L., and P. A. Demkowicz. 2023. “AGR TRISO Fuel Fission Product Release Data Summary.” INL/RPT-23-74651, Idaho National Laboratory, Idaho Falls, ID.

Stempien, J. D. and L. Cai. 2024a. “Radial Deconsolidation and Leach-Burn-Leach of Eight As-Irradiated AGR-3/4 TRISO Fuel Compacts.” INL/RPT-24-77357, Idaho National Laboratory, April 2024.

Stempien, J. D. and L. Cai. 2024b. “Radial Deconsolidation Leach-Burn-Leach of Five AGR-3/4 TRISO Fuel Compacts after Post-Irradiation Heating Tests.” INL/RPT-24-80406, Idaho National Laboratory, September 2024.

Sterbentz, J.W. 2015. “JMOCUP As-Run Daily Physics Depletion Calculation for the AGR-3/4 TRISO Particle Experiment in ATR Northeast Flux Trap.” Rev. 1, ECAR-2753, Idaho National Laboratory, July 2015.